이학석사 학위논문

중심립-중심체 전환과정의 핵심요소인 CEP152의 세포분열기에서 조절기전 연구

Studies on mitotic regulation of CEP152, a critical factor for centriole-to-centrosome conversion

2019년 8월

서울대학교 대학원

생명과학부

김 정 진

ABSTRACT

To regulate the number of centrosomes, only one daughter centriole can grow on a mother centriole at once. The daughter centriole needs to become a new mother centriole to be a platform for a new centriole duplication. This process becoming a mother centriole from a daughter centriole is called centriole-to-centrosome conversion. In early G1 phase of a human cell, CEP152 is localized at converted centriole and the localization of CEP152 is important for centriole assembly. Most of the researches about CEP152 in conversion has focused on the cell cycle after mitotic exit, so regulation of CEP152 with entering mitosis hasn't been reported. Here I report that centrosomal CEP152 localization is regulated by Plk1 activity through a regulation of the interaction between CEP152 and its candidate proteins in mitosis. In addition, I show that a domain for centrosomal localization of CEP152 changes with entering mitosis. Furthermore, I propose clues to connect centrosomal CEP152 regulation in mitosis with centriole-to-centrosome conversion by investigation of CPE152 domain and its interaction partner shifting.

CONTENTS

LIST OF FIGURES

Background

1. Composition of centrosome

The centrosome is a membraneless organelle, composed of two centrioles arranged at a perpendicular angle to each other, and surrounded by a non-crystalline mass of proteins called pericentriolar material (Bettencourt-Dias and Glover, 2007).

1.1 Centriole

This centriole has a cylindrical structure made up of nine-triplet microtubules (Fig. 1). The length and diameter of centriole is approximately 500 nm and 250 nm for each (Gönczy, 2012). There are two types of centriole, mother centriole, and daughter centriole. At the beginning of S phase in cells, a daughter centriole is synthesized from the wall of a mother centriole in right-angle position.

1.2 Pericentriolar material

The pericentriolar material (PCM) is a protein complex surrounding centriole. Pericentrin, CDK5RAP2/CEP215, CEP192 and γ-tubulin are well known PCM proteins (Lawo et al., 2012) (Fig. 2). These PCM proteins recruit γ-tubulin ring complex (γ-TuRC) for centrosome to have proper function (Kollman et al., 2011). Its size varies throughout cell cycle, for instance, the size increases a lot due to PCM maturation

when cells are getting into mitosis (Kim and Rhee, 2014).

2. Function of centrosome

2.1 Microtubule nucleation

Centrosome is an organelle in cells which has a function for microtubule organization because the pericentriolar material has a large amount of γ-TuRC which is the core functional unit for microtubule nucleation(kollman et al., 2011). This is a reason why centrosome is so-called MicroTubule Organizing Center (MTOC) (Conduit et al., 2015). Because of its ability to organize microtubule nucleation in cells, centrosome forms microtubule network through interphase and has an important role in spindle pole formation in mitosis. Microtubule network is needed for maintaining cell shape, cell migration, and intracellular transport (Hardin et al., 2012) (Fig. 3). When cells are getting into mitosis, PCM maturation also known as centrosome maturation occurs with PCM expansion by recruiting PCM proteins. This enables cells to have efficient microtubule nucleation activity for chromosome segregation by spindle formation in mitosis.

2.2 Primary cilia formation

In addition to its role as MTOC, centrosome can become a basal body and forms primary cilia which has critical roles in signal transduction in cells (Wheway et al., 2018).

3. Centrosome cycle

Centrosome is duplicated once per cell cycle through series of processes as well as DNA and this is called centrosome cycle. Centrosome cycle is divided into 5 steps (Wang et al., 2014) (Fig. 4).

First step is centriole duplication initiation which begins at cell's entering S phase. Newly synthesized daughter centriole, which is also called procentriole, grows in perpendicular angle from mother centriole's wall. This daughter centriole is unable to synthesize other centrioles on its wall. When a mother centriole is tightly engaged to daughter centriole, this mother centriole loses its ability to form another daughter centriole and this is an important licensing mechanism for centriole duplication.

Second step is centriole elongation. After the initiation of centriole, a daughter centriole elongates its lengths until Mitosis. Normally it grows about 500nm.

Third step is centrosome maturation and separation. This step is necessary for centrosome to have a role as mitotic spindle. Mitotic PCM is three to five times larger than Interphase PCM and this PCM expansion maximizes centrosome's microtubule nucleation activity. When cells are getting into mitosis, linker proteins are removed, and two centrosomes are separated to each side of cell.

Forth step is bipolar spindle assembly. A Centrosome in this step can form spindle fiber to segregate chromosome concisely through Mitosis.

Last step is centriole disengagement. When one cell is divided into two cells by cytokinesis, each cell has one centrosome with two centrioles. At this point, daughter centriole is disengaged from mother centriole and becomes young mother centriole by centriole to centrosome conversion.

4. Centriole to centrosome conversion

4.1 Conversion: a daughter centriole becomes a mother centriole

Final step of centrosome cycle is centriole disengagement followed by centriole to centrosome conversion. When daughter centriole is converted to mother centriole, this young mother centriole can be a platform for new daughter centriole duplication initiation. Also, this young mother centriole can recruit PCM proteins to form PCM. Plk1 activity in mitosis and centriole disengagement are pre-requisite for this conversion (Wang et al., 2011) (Fig. 5). Activation of separase in addition to Plk1 is also needed for centriole disengagement (Tsou et al., 2009). On top of that, pericentrin needs to be cleaved by separase for the conversion (Kim et al., 2019a).

4.2 CEP152 as conversion factor

It is possible to notice whether a centriole is converted or not by observing CEP152 localization and therefore, CEP152 is called conversion factor. A series of centrosome protein recruitment occurs through conversion process. Other conversion factors, such as CEP135, CEP295, CEP192, also needs to exist for daughter centriole to be converted to mother centriole. But other conversion factors, except CEP152, are located at daughter centriole even before exiting mitosis. Since CEP152 is manly associated with Plk4, which is key regulator for centriole duplication, localization of CEP152 at a centriole after exiting mitosis has strong indicator for conversion (Fu and Glover, 2016; Izquierdo et al., 2014).

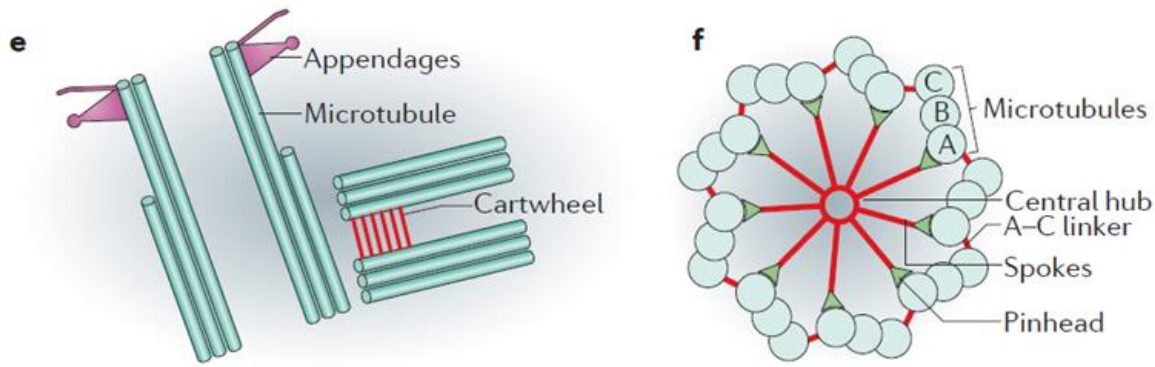

Figure 1. Schematic representation of human centrosome The centrosome is composed of one to two centriole which consists of nine microtubule triplets. One triplet consists of A, B, and C microtubules. Centriole has cylindrical structure and a mature mother centriole has appendages on its distal end. Only daughter centriole has cartwheel structure. (Gonczy, 2012)

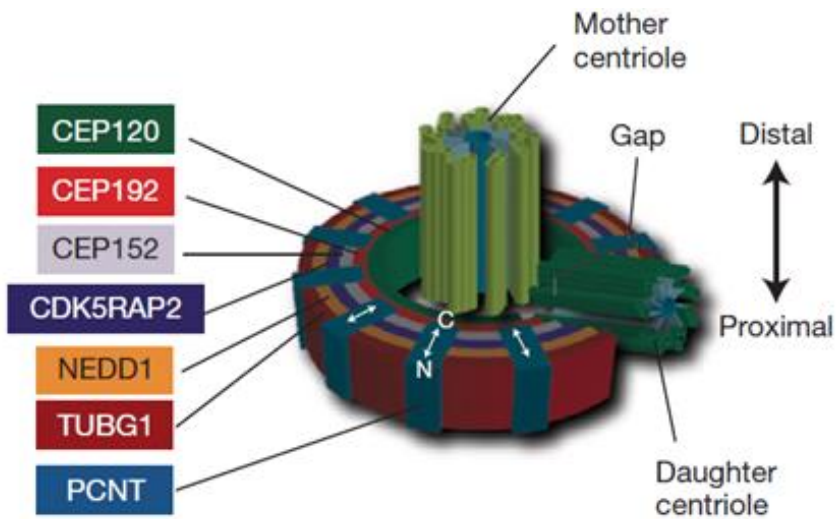

Figure 2. Structure of pericentriolar material (PCM) Proximal end of mother centriole is surrounded by PCM and PCM proteins are arranged in specific order. Only mother centriole converted from daughter centriole can recruit PCM proteins to form this toroidal structure PCM. (Lawo et al., 2012)

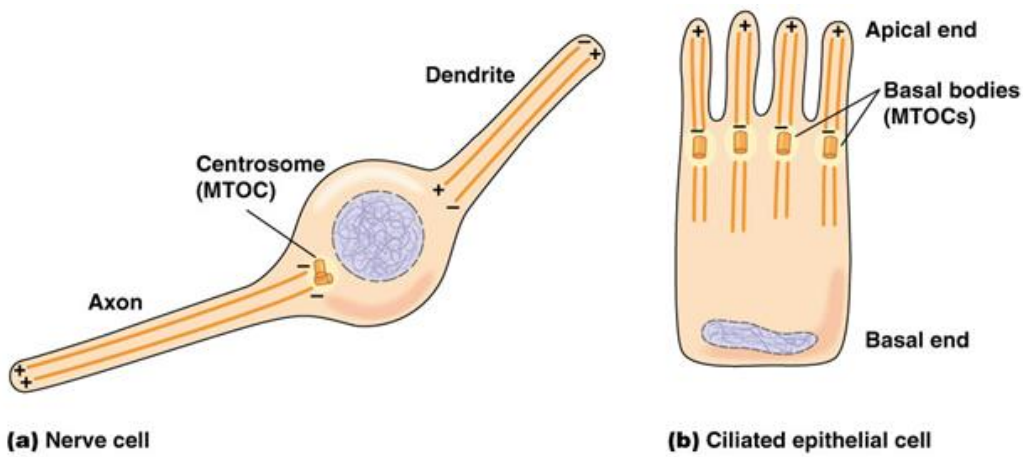

Figure 3. Function of centrosome in interphase Centrosome is an organelle in cells for microtubule nucleation and called as microtubule organizing center (MTOC). Its microtubule nucleating activity is essential for maintaining cellular morphology. (Hardin et al., 2012)

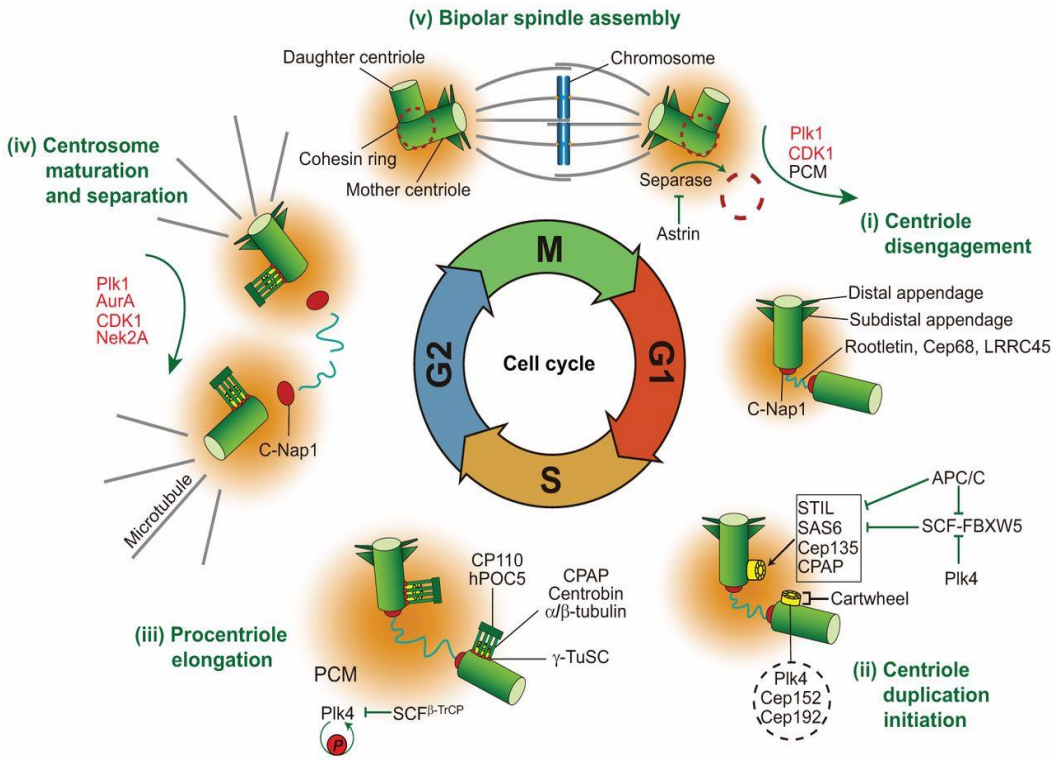

Figure 4. Centrosome cycle Centrosome is duplicated once per cell cycle by following centrosome cycle. Centrosome cycle is composed of centriole duplication initiation, centriole elongation, centrosome maturation and separation, Bipolar spindle assembly, and centriole disengagement. (Wang et al., 2014)

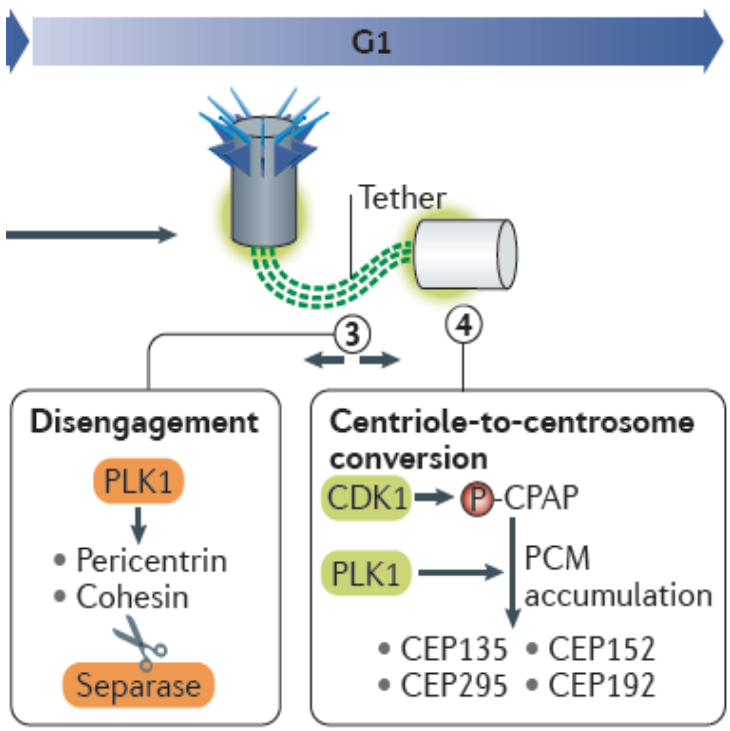

Figure 5. Centriole to centrosome conversion Once a daughter centriole is converted to mother centriole, this new converted mother centriole is able to recruit PCM proteins and to be a platform for a new daughter centriole duplication. Activation of CDK1 and PLK1 is essential for this centriole to centrosome conversion process and CEP152 is a key conversion factor. (Nigg and Holland, 2018)

INTRODUCTION

The centrosome is a cylindrical organelle composed of centriole and pericentriolar material (PCM) surrounding a proximal end of mother centriole (Bornens, 2012). Main function of centrosome is microtubule nucleation, and this is a reason for the centrosome to be called microtubule organizing center, MTOC. The number of centrosomes must be tightly regulated through whole cell cycle by following centrosome cycle. The centrosome needs to be duplicated only once per cell cycle (Wang et al., 2014). Otherwise, centrosome aneuploidy can cause chromosome instability (CIN) which eventually can lead to a cancer development (Holland and Cleveland, 2009).

When a centrosome duplication is initiated from S phase, new centriole called procentriole or daughter centriole grows from the wall of mother centriole mainly by Plk4, the regulator kinase of centriole duplication (Habedanck et al., 2005). This growing centriole is blocking another centriole duplication initiation from the other side of mother centriole, which is a licensing mechanism for only one centriole duplication from one mother centriole (Nigg, 2007). Also, daughter centriole can't be a platform for a centriole duplication and that is the reason for only one centriole formation from a mother centriole. After the daughter centriole fully grown and cells entering mitosis, two

centrosomes consist of two centriole each are separated and divided into two daughter cells (Wang et al., 2014). When cells are exiting mitosis, a daughter centriole is disengaged from a mother centriole and becomes a mother centriole by conversion (Wang et al., 2011). This young mother centriole is capable of recruiting PCM proteins and being a platform for new centriole growing (Wang et al., 2011). To enter a new round of centriole duplication by Plk4, CEP152 needs to be located at converted mother centriole. Without CEP152, centriole initiation cannot be started, and therefore CEP152 is an indicator for a conversion. By observing a localization of CEP152, it is possible to know which centriole is converted and becomes mother centriole (Dzhindzhev et al., 2010).

Many CEP152 interaction partner proteins have been studied and revealed, such as CEP63, CEP192, CEP295, CPAP and Plk4 (Brown et al., 2013; Cizmecioglu et al., 2010; Fu et al., 2016; Hatch et al., 2010; Kim et al., 2019b; Sonnen et al., 2013). Additionally, more interaction proteins were revealed by Bio-ID, such as SAS6, CEP128, CNTRL, CEP135, CEP120, POC5 (Gupta et al., 2015). Although many researches were carried out and have revealed some of mechanisms involving CEP152 and protein-protein interactions of CEP152 with other proteins, whole regulation mechanism of CEP152 still remain unclear. Especially, a regulatory mechanism of CEP152 in mitosis hasn't been reported yet.

Plk1 is a kinase which has many roles throughout cell cycle as

known as all round player. One of the well-known roles is modifying a daughter centriole to become a mother centriole through mitosis (Wang et al., 2011). Also, artificial activation of Plk1 in S phase arrested cells caused uncontrolled conversion and centriole overduplication (Lončarek et al., 2010). On top of that, recent research has revealed that making Polo/Plk1's docking site with phosphorylating Thr200 of Sas4/CPAP by cdk1 is essential for centriole to centrosome conversion (Novak et al., 2016). Surely, plk1 has crucial function in conversion mechanism.

In this report, I claim that Plk1 regulates centrosomal CEP152 level by altering CEP152's protein-protein interaction in mitosis. Besides, I suggest a concept about interaction partner shifting of CEP152 which alludes clues to reveal a specific regulatory mechanism of CEP152 in conversion. Eventually, I propose a model to explain centrosomal CEP152 level reduction with cell's entering mitosis regulated by plk1 kinase activity.

MATERIALS AND METHODS

Cell culture and cell cycle synchronization

The Flp-In T-REx HeLa cells and HEK 293T cells were cultured in DMEM (Welgene, LM 001-05) supplemented with 10% FBS (Welgene, S101-01) and antibiotics (Invivogen, ANT-MPT) at 37℃ and 5% CO2. All cell lines were regularly tested for mycoplasma contamination test with mycoplasma PCR detection kit (CellSafe, CS-D-50). To synchronize cell cycle, I used 2 mM thymidine (Sigma-Aldrich, T9250), 5 μM paclitaxel (Taxol, Sigma-Aldrich, T7402), 5 μM RO-3306 (Enzo Life Sciences, ALX-270-463-M005) and 2 mM ZM447439 (Cayman chemical company, 13601). For inhibition of PLK1 activity during mitosis, I treated the cells with 100nM BI2536 (Selleck chemicals, S1109) for 3 h after the thymidine–paclitaxel block.

Plasmids, siRNA transfection

All CEP152 (NCBI reference sequence: NM_014985.4) constructs were subcloned into p3xFLAG-CMV-10 vector (Sigma-aldrich, E7658) tagged with 3xFLAG at 5′ end. All CEP152 interaction proteins (CEP63, CEP192, CEP295, CPAP and Plk4) constructs were subcloned into pCMV-tag-3A vector (Agilent Technologies) tagged with Myc at 3′ end, except

CEP295 tagged at 3′ end). To generate siRNA-resistant CEP152 construct, I induced silent mutations of CEP152 with the following primers: 5′- ATT CAG CTC GAG ATT -3′ and 5′- AAT CTC GAG CTG AAT -3′. For depletion of endogenous CEP152, CEP63, CEP192, CEP295 and CPAP, siCEP152 (5′ - GCG GAU CCA ACU GGA AAU CUA -3′), siCEP63 (5′ - CGU CAG AAA UCG CUG GAC U -3′), siCEP192 (5′ - GGA AGA CAU UUU CAU CUC U -3′), siCEP295 (5′ - GUG AUA CAC UAA CAA UUG A -3′) and siCPAP (5′ - GGA CUG ACC UUG AAG AGA A -3′) were used. A scrambled siRNA sequence (siCTL; 5′ - GCA AUC GAA GCU CGG CUA CTT -3′) was used as a control. Lipofectamine 3000 and RNAiMAX (Invitrogen) were used for DNA transfection and siRNA transfection according to the manufacturer's protocol.

Antibodies

The CEP135 (ICC 1:2,000) (Kim et al., 2008), PCNT (ICC 1:5,000, IB 1:2,000) (Kim and Rhee, 2011) and CPAP (ICC 1:100) (Chang et al., 2010) antibodies were previously described. Antibodies specific to GFP (Santa Cruz Biotechnology, sc-9996; ICC 1:500), FLAG (Sigma-Aldrich, F3165; ICC 1:2000, IB 1:20,000), centrin-2 (Merck Millipore, 04-1624; ICC 1:1,000), CEP295 (Abcam, 122490; ICC 1:500, IB 1:250), CEP192 (Bethyl Laboratories, A302-324A; ICC 1:1,000, IB 1:250), CEP152 (Abcam, 183911; ICC 1:1,000, IB 1:500), GAPDH (Life Technologies, AM4300; IB 1:20,000),

γ-tubulin (Abcam, 11316; ICC 1:1,000) and Plk4 (Millipore, MABC544; ICC 1:100, IB 1:250) were purchased. The secondary antibodies conjugated with fluorescent dye (Alexa-488, Alexa-594, Alexa-647; Life Technologies, ICC 1:1,000) and with horseradish peroxidase (Sigma or Millipore, IB 1:10,000) were purchased.

Establishments of inducible CEP152-PACT proteins expression and degradation system

To regulate CEP152-PACT proteins expression and degradation, I simultaneously applied *pcDNA™5/FRT/TO* and ProteoTunerTM systems. Four FLAG-CEP152-PACT constructs were attached with destabilization domain of pTRE-Cycle1 vector (Clontech Laboratories, 631115) and subcloned into pcDNA™5/FRT/TO vector (Invitrogen, V6520-20). To induce Flp recombinase-mediated integration, pOG44 (Invitrogen, V6005-20) and *pcDNA™5/FRT/TO* vectors containing Flag-CEP152-PACT construct were cotransfected to Flp-In T-REx HeLa cells. DNA transfection was performed with Lipofectamine 3000 (Invitrogen) according to manufacturer's protocol. After transfection, 0.1 mg/ml Hygromycin B (Calbiochem, 400051) were treated for 2-3 weeks and then polyclonal cell lines were established. To induce and stabilize ectopic CEP152-PACT proteins, 10 ng/ml doxycycline (Sigma-Aldrich, D9891) and 50 nM shield1 (Clontech Laboratories, 632189) were treated.

Immunoblot analyses

The cells were lysed on ice for 10 min with RIPA buffer (150mM NaCl, 1% Triton X-100, 0.5% sodium deoxycolate, 0.1% SDS, 50 mM Tris-HCl at pH 8.0, 10mM NaF, 1mM Na3VO4, 1mM EDTA and 1mM EGTA) containing a protease inhibitor cocktail (Sigma-Aldrich, P8340) and centrifuged with 12,000 rpm for 10 min at 4℃. The supernatants were mixed with 4 × SDS sample buffer (250mM Tris-HCl at pH 6.8, 8% SDS, 40% glycerol and 0.04% bromophenol blue) and 10 mM DTT (Amresco, 0281-25G). Mixtures were boiled for 5 min. 15–20 mg of proteins were loaded in SDS polyacrylamide gel (3% stacking gel and 4% separating gel or 5% stacking gel and 6 % separating gel), electrophoresed and transferred to Protran BA85 nitrocellulose membranes (GE Healthcare Life Sciences, 10401196). The membranes were blocked with blocking solution (5% nonfat milk in 0.1% Tween 20 in TBS or 5% bovine serum albumin in 0.1% Tween 20 in TBS) for 2 h, incubated with primary antibodies diluted in blocking solution for 16 h at 4℃, washed four times with TBST (0.1% Tween 20 in TBS), incubated with secondary antibodies in blocking solution for 30 min and washed again. To detect the signals of secondary antibodies, ECL reagent (ABfrontier, LF-QC0101) and Xray films (Agfa, CP-BU NEW) were used. In the cases of other proteins, 5% stacking and 10-18% separating gels were used.

Immunostaining analysis

For immunocytochemistry, cells seeded on cover glass (Marienfeld, 0117520) were fixed with cold methanol for 10 min and washed three times with cold PBS. After incubation of PBST (0.1% Triton X-100 in PBS) for 10 min, the cells were blocked with blocking solution (3% bovine serum albumin, and 0.3% Triton X-100 in PBS) for 30 min, incubated with primary antibodies diluted in blocking solution for 1 h, washed three times with PBST, incubated with secondary antibodies in blocking solution for 30 min, washed twice with PBST, incubated with 4,6-diamidino-2-phenylindole (DAPI) solution for 3 min and washed twice with PBST. The cover glasses were mounted on a slide glass with ProLong Gold antifade reagent (Life Technologies, P36930). Images were acquired from fluorescence microscopies equipped with digital cameras (Olympus IX51 equipped with QImaging QICAM Fast 1394 or Olympus IX81 equipped with ANDOR iXonEM+) and processed in ImagePro 5.0 (Media Cybernetics). Adobe photoshop CS6 was used in order for pseudo-coloring. To measure fluorescence intensities, I immunostained all cells at the same time with same diluent antibodies. All images were captured at same exposure time without stopping. Image J 1.51k was used to measure fluorescence intensities at centrosomes. In each measurement, background signals were subtracted from the sum of fluorescence signals

at centrosomes.

Immunoprecipitation

For coimmunoprecipitation experiments, HEK293T cells were transfected with DNA constructs using PEI. The cells were treated with cell cycle synchronization drugs following the experiment schemes (Fig. 16a; Fig. 19a), and lysed on ice for 20 min with a lysis buffer (25 mM Tris-HCl [pH 7.4], 100 mM NaCl, 5 mM MgCl2, 5 mM NaF, 20 mM b-glycerophosphate and 0.5% NP-40) containing an appropriate amount of protease inhibitor cocktail (P8340; Sigma-Aldrich). The lysates were centrifuged at 12,000 rpm for 20 minutes at 4uC, and the supernatants were incubated with FLAG-M2 AffinityGel (A2220; Sigma-Aldrich) for 1.5 h at 4℃. The immunoprecipitates were then used for immunoblot analyses.

Statistical analysis

For statistical analyses, experiments were independently performed two to three times. To calculate P values, unpaired two-tailed t-test, one-way analysis of variant (ANOVA) were performed in Prism 6 (GraphPad Software). In the case of ANOVA, the Tukey's or Sidak's multiple comparisons test was performed if p value is lower than 0.05.

All measured fluorescent intensities were displayed with box-and-whiskers plots in Prism 6 (lines, median; vertical boxes, values from 25th and 75th; down error bars, 10th value, up error bar, 90th value; circle, outliers).

RESULTS

PLK1 regulation of the centrosomal CEP152 levels during onset of mitosis

In order to determine centrosomal level of CEP152 in cells entering mitosis, HeLa cells were arrested in S phase by thymidine block for 20 h, released in the presence of paclitaxel, and harvested them at 0, 5 and 10 h later (Fig. 6a). Since it is known that pericentrin (PCNT) accumulates into the centrosome entering mitosis and is cleaved during mitotic exit (Lee and Rhee, 2012; Matsuo et al., 2012), PCNT was used as an indicator for mitotic cells along with cyclin B1 (Fig. 6b). I measured the intensities of centrosomal PCNT and CEP152 in 3 groups fixed at 3 different time points and PCNT level increased as it had been already known. On the contrary, the centrosomal CEP152 levels decreased when cells entered mitosis (Fig. 6c, d, e). On top of that, amount of CEP152 decreased also in total cell lysates.

Plk1 is a major regulator for PCM maturation which makes PCNT level higher at the onset of mitosis. BI2536, a PLK1 inhibitor, was treated in mitotic cells and determined expression of CEP152 (Kim and Rhee, 2014; Fig. 7a). As expected, BI2536 treatment reduced centrosomal levels of PCNT (Fig. 7c, e). On the contrary, the centrosomal levels of CEP152

significantly increased in the BI2536-treated cells, even though the total amount of CEP152 proteins did not change (Figs. 2b-d). These results suggest that the centrosomal levels of CEP152 is regulated by PLK1 at the onset of mitosis.

Definition of CEP152 domains for centrosomal localization and PLK1 regulation

Some studies have revealed functions of domains in CEP152, such as domains responsible for centrosomal localization and protein-protein interaction. However, CEP152's domains related to PLK1-associated centrosomal level regulation has not been reported. Several CEP152 truncated mutants were generated by Site-directed Mutagenesis to perform domain studies (Fig. 8a). Ectopic CEP152 mutants were expressed in cells by transient transfection and these cells were arrested in mitosis by using thymidine and Taxol (Fig. 7b). Similar to the tendency of endogenous CEP152, the amount of these ectopic deletion mutants decreased in total cell lysates when cells were getting into mitosis (Fig. 7c). For the centrosomal level, most of mutants showed similar level but Δ5 mutant couldn't be localized to centrosome as known in a previous report (Hatch et al., 2010; Fig. 8d, e). Δ1 mutant had little bit of higher centrosomal level in both cells. Δ2 and Δ3 mutants showed similar centrosomal levels in both cells. Otherwise, even though Δ4 and Δ6

mutants had similar centrosomal level in Interphase cells, they showed lower centrosomal level in cells arrested at prometaphase(Fig. 8d, e, f)

Like an endogenous CEP152 again, it was obvious that BI2536 didn't change the amount of expression level in total lysates just like endogenous CEP152(Fig. 9a, b, c). Although ectopic CEP152 Full length, Δ1, Δ2 and Δ3 deletion mutants showed centrosomal level increment after BI2536 treatment as same tendency as endogenous CEP152, Δ4, Δ 5 and Δ6 deletion mutants didn't showed centrosomal level increment after BI2536 treatment (Fig. 9d, e). Even though Δ4 and Δ6 mutants were able to be localized at the centrosome in interphase, these ectopic CEP152 truncated mutants were barely detected at the centrosome like Δ5 mutant in mitosis(Fig. 8d, f), and they couldn't be involved in centrosomal level increment induced by Plk1 inhibition. This result indicates that a CEP152's domain responsible for centrosomal localization in interphase might be different with a domain for centrosomal localization in mitosis and a domain related to PLK1 regulation.

To make sure which domains were important for this centrosomal localization in each cell cycle and centrosomal level increment induced by BI2536 treatment, few more combination of CEP152 deletion fragments related to Δ4, Δ5 and Δ6 were generated (Fig. 10a). After checking out their expression by immunoblot analyses (Fig. 10b), their centrosomal localization were also checked by coimmunostaining

analyses (Fig. 10c). Only CEP152 Δ5 mutant out of 6 CEP152 truncated mutants couldn't be localized at the centrosome (Fig. 8a, d, e), besides, #5 and other little bit longer fragments, such as #5+Ala, #5++ couldn't be localized at the centrosome. Also, neither could #4 and #6 (Fig. 10c). Since #4+5, #5+6 and #4+5+6 could be localized at the centrosome, although #4+5 and #5+6 showed weak signal, centrosomal intensities of these ectopic CEP152 deletion fragments were measured in BI2536 treated condition (Fig. 11a). As a result, #4+5+6 deletion fragment was the minimum fragment which could be localized at the centrosome in interphase and mitosis. Also, it had an increased centrosomal level induced by BI2536 treatment (Fig. 11b, c).

By these series of experiment with CEP152 mutants, I found out clear fact that a domain located within number 5 region (1045-1289aa) was necessary but not sufficient for centrosomal localization. And number 4, 5 and 6 regions were necessary for centrosomal localization in mitosis and centrosomal level increment induced by BI2536 treatment. These results suggest that the important domains for centrosomal localization are changed through a cell cycle. Since the reason for centrosomal localization is most likely due to protein-protein interactions, this alteration of the important domain for centrosomal localization with entering mitosis possibly means the alteration of the domain related to protein-protein interactions.

When it comes to a minimum domain for centrosomal localization of CEP152, there was a report claimed that #5+Ala (1045-1290aa) was necessary and sufficient for centrosomal localization and it is different from my experiment result (hatch et al., 2010). A difference of experimental scheme was Tag on 5′ of CEP152. GFP tag was attached in other group and Flag in my research. So, Flag tag for my mutants were substituted with EGFP tag. Interestingly, #5 and #5+Ala small fragments were able to be localized at the centrosome (Fig. 12a). Furthermore, it has been revealed that much smaller CEP152 fragment 1205-1272aa was able to be localized at the centrosome with co transfection of CEP63(Kim et al., 2019). So I performed a similar experiment with co-transfection of CEP63 and CEP152 deletion mutant using HeLa cells and HEK293 T cells, and as expected, small CEP152 deletion fragment was spotted at the centrosome (Fig. 12b). These results indicate that CEP152 interaction with CEP63 is important for centrosomal localization of the CEP152-CEP63 complex (Kim et al., 2019). Also, CEP152's dimerization might be an important factor too because GFP has a tendency to self-dimerize at high concentrations (Chalfie and Kain, 2005).

Regulation of CEP152 interactions with specific centrosomal proteins during cell cycle

To verify the hypothesis that interaction partners of CEP152

change throughout cell cycle, series of co-immunoprecipitation experiments were performed with 5 interaction candidates, which were CEP63, CEP192, CEP295, Plk4 and CPAP. Protein-protein interaction of CEP152 and these interaction candidates were already confirmed by several researches (Brown et al., 2013; Cizmecioglu et al., 2010; Fu et al., 2016; Hatch et al., 2010; Kim et al., 2019b; Sonnen et al., 2013). These proteins were fused with Myc tag because Flag tag was already attached at 5′ of CEP152. After the expression check by Immunocytochemistry and Immunoblot analyses (Fig. 13), co-IP experiments were performed. Plk4 were co-immunoprecipitated with CEP152 well, but CPAP were not for the first experiment (Fig. 14). CPAP was well co-immunoprecipitated in the next experiment and the other proteins were too, which were CEP63, CEP192 and CEP295 (Fig. 15).

To determine protein-protein interaction of CEP152 and other proteins throughout cell cycle, HEK 293T cells were synchronized to G2 phase by 8 h of RO3306 treatment, prometaphase by 10 h of Taxol treatment and G1 phase by treating ZM447439 for the cells to be forced to exit mitosis, following to 16 h of thymidine treatment 4 h after co-transfection of CEP152 and interacting proteins (Fig. 16a). Cell synchronization was checked by CyclinB1 level, which is getting higher with cells' entering mitosis and is getting lower with exiting mitosis, and microscopic observation of cell morphology. These co-IP immunoblot analysis were performed twice independently. CEP63 repeatedly showed

similar band pattern in all groups (Fig. 16b). Plk4 band was more intense in untreated asynchronous group (Fig. 16c), which might mean that the interaction of Plk4 and CEP152 is stronger in other cell cycle than G2/Mitosis/G1, such as S phase. For CEP295, two independent experiments showed little bit different results in ZM447439 treated group. However, it is same for both experiments that CEP295 bands were getting weaker when cells were getting into mitosis by Taxol treatment (Fig. 17a). Coimmunoprecipitated CPAP showed similar pattern repeatedly that CPAP band was getting weaker in Taxol and ZM447439 treated group (Fig. 17b). The result of CEP192 co-IP experiment is hard to interpret because their expression level kept changing throughout cell cycle and its band pattern was not same for each experiment. But still, CEP192 was well co-immunoprecipitated by CEP152 repeatedly in RO3306 treated group even though the amount of input CEP192 was low in this group (Fig. 18).

Since BI2536 treatment made centrosomal CEP152 level higher at prometaphase, co-IP experiment with these interaction candidates were performed in BI2536 treated condition. HEK 293T cells were arrested in prometaphase by Thymidine and Taxol treatment followed by BI2536 treatment (Fig. 19a). For CEP63, CEP295, Plk4 and CPAP, their band patterns were almost same in DMSO control group and BI2536 treated group (Fig. 19a, b, c, d, e). Also, their tendency of untreated group and Taxol treatment group in previous experiment (Fig. 16, 12, 13) were well

repeated here correspondent to untreated group and DMSO group in Figure 14. In other words, weaker band patterns in prometaphase were also observed repeatedly in both CEP295 and CPAP. Interestingly, protein-protein interaction between CEP192 and CEP152 was getting stronger with BI2536 treatment (Fig. 19f).

These analyses were carried out in proteins' overexpressed condition and it is hard to say that these interaction observations between proteins were specific to centrosomal interaction. Nevertheless, these results of co-IP experiment suggest that some protein-protein interactions could change throughout cell cycle. Especially, interaction weakening of CEP152 with CEP295 and CPAP in mitosis are quite noticeable results. In addition, the result of strong interaction between CEP63 and CEP152 supported the hypothesis that CEP63-CEP152 complex is essential for centrosomal localization in both of interphase and mitosis.

Depletion of specific interaction proteins affects the centrosomal levels of CEP152

If an interaction between CEP152 and specific protein is the main reason for centrosomal localization, depletion of the protein would cause centrosomal CEP152 level reduction. Therefore, centrosomal CEP152 level observations after depletion of CEP152 interaction proteins were carried

out by coimmunostaining and immunoblot analyses. First, siRNA knockdown efficiency tests were performed (Fig. 20). Due to unavailability of CEP63 antibody, the test was carried out with CEP63-Myc transfection. After checking out their knockdown efficiency, HeLa cells were arrested at prometaphase using Thymidine and Taxol, and centrosomal CEP152 levels were measured (Fig. 21). Centrosomal levels of CEP152 after treating CEP63 were lower than control in both of Interphase and prometaphase cells. Unexpectedly, depletion of CEP192 made centrosomal CEP152 levels higher in both groups. Because of a previous report that CEP192 knockdown causes CEP152 to decrease in interphase cells and especially in S phase (Brown et al., 2013; Sonnen et al., 2013), this CEP152 level increment in prometaphase was quite surprising. Depletion of CEP295 and CPAP didn't make statistically significant differences in Interphase cells, on the other hand, statistically significant reductions of centrosomal CEP152 were observed in prometaphase arrested cells.

After comparing Interphase cells and prometaphase cells with siRNA treatment, centrosomal CEP152 levels were measured in BI2536 treated mitotic cells (Fig. 22). When CEP63 was depleted in cells, a centrosomal CEP152 level increment was not significant. Depletion of CEP192 made centrosomal CEP152 level as similar as BI2536 treated control group in both of DMSO treated and BI2536 treated groups. Either CEP295 depleted or CPAP depleted groups had increment of centrosomal

CEP152 levels with BI2536 treatment, but their centrosomal CEP152 levels were lower than that of control group with BI2536 treatment.

From these results, it is obvious the interaction between CEP152 and CEP63 is fundamental basis for centrosomal localization. And CEP152's interaction with CEP295 and CPAP is likely to be a reason for centrosomal localization of CEP152 in mitosis because the depletions of CEP295 and CPAP only affected centrosomal CEP152 levels in mitosis, not in interphase. For CEP192, the effect of CEP192 depletion on centrosomal CEP152 level was similar as BI2536 treatment, and this result suggests that CEP192's function might be related to Plk1 kinase regulation on centrosomal CEP152.

Specific interaction of CEP152 with CEP63 is essential for centriole assembly in the next round

PACT is a domain from Pericentrin, which is known for its centrosomal localization function (Gillingham and Munro, 2000). Recently, it is known that the reason for PACT domain's ability to centrosomal localization is due to the interaction between PACT and CEP57, one of the centrosomal proteins (Watanabe et al., 2019). So, attaching PACT domain on a protein makes it possible for the protein to be localized at the centrosome. Two new truncated CEP152-PACT were made by combining PACT domain on 3′ of CEP152 full length and Δ5 truncated

mutant, which couldn't be localized at centrosome (Fig. 23a). As expected, all constructs were well expressed in HeLa cells after transfection and Flag-CEP152 Δ5-PACT was able to be localized at the centrosome, on the other hand, Flag-CEP152 Δ5 was not (Fig. 23b, c).

In order to observe behaviors of these four constructs under the circumstance of endogenous CEP152 depletion, siCEP152 was treated and cells were arrested at prometaphase using thymidine and Taxol after transfection (Fig. 24a). Cells had a wide range of ectopic CEP152 levels for every construct and some cells had strong CEP152 intensities even at prometaphase (Fig. 24b).

To overcome the limitation of transient transfection system which had too various expression levels, 4 truncated Flag-CEP152-PACT proteins were cloned into another vector to make FRT/TO stable cell line. Theoretically, every cell is supposed to have the same amount of expression level because FRT/TO HeLa cell would uptake only one copy of ectopic protein gene and promoter. Also, the expression level of this protein could be tightly controlled by two factors. The expression of this ectopic protein could be initiated by doxycycline treatment and it would be degraded without shield1 treatment because of the addition of a destabilization domain (DD) (Banaszynski et al., 2006; Egeler et al., 2011). After a selection process for FRT/TO stable cell lines, expressions were checked by coimmunostaining and immunoblot analyses (Fig. 25).

Unexpectedly, every single cell didn't have a same amount of centrosomal CEP152 even thought they were all siRNA resistant. Their total expression levels were also too lower than endogenous CEP152 level.

Before performing phenotypic analyses, co-IP experiment with CEP63-Myc and truncated Flag-CEP152-PACT proteins was performed because it had already been reported that the small region in #5(1045-1289aa) of CEP152(1-1654aa) was necessary for interaction with CEP63 (Kim et al., 2019b). Expectedly, Flag-CEP152 full length and Flag-CEP152 full length–PACT proteins were able to interact with CEP63, on the other hand, Flag-CEP152 Δ5 and Flag-CEP152 Δ5–PACT proteins were not (Fig. 26).

In order to test whether these truncated Flag-CEP152-PACT proteins have proper function, the number of SAS6 was counted after endogenous CEP152 depletion. It was known that depletion of CEP152 caused for cells to lose their SAS6 foci because CEP152 is a licensing factor for initiating centriole duplication initiation and sas6 is recruited to centriole duplication initiation site to form new centriole (Kitagawa et al., 2011; Novak et al., 2014). Since setting up stable cell lines was quite unsuccessful because the cell lines had too low ectopic protein expression level compared to endogenous CEP152, transient transfection was also used for phenotypic analysis. CEP152 depleted cells were

induced to express truncated Flag-CEP152-PACT proteins by two means, transient transfection and doxycycline plus shield1 (Fig. 27). Despite their bipolar expression level, too high or too low, tendencies were pretty much same for both conditions. Most of cells had 2 SAS6 dots in control group and many cells no longer had SAS6 dots after depletion of CEP152 in correspondence with previous researches. Even though Flag-CEP152 Full length and Flag-CEP152 Full length–PACT couldn't rescue this phenotype fully, the percentage of cells with 2 SAS6 dots was increased and cells with 0 SAS6 dots was decreased compared to siCEP152 treated group. Cells with Flag-CEP152 Δ5 and Flag-CEP152 Δ5–PACT had almost same tendency to siCEP152 treated group, which meant those cells were not rescued at all.

As a result, CEP152 needs to interact with CEP63 to have a proper centriole assembly activity regardless of its centrosomal localization.

DISCUSSION

All my experiments were started from the interesting observation of CEP152's opposite behavior when cells were entering mitosis. Centrosome maturation process makes PCM larger by recruitment of PCM proteins. Since Plk1 regulates this PCM expansion, inhibition of Plk1 also inhibits PCM expansion process, and centrosomal intensities of PCM proteins decreases by BI2536 treatment. On the contrary, centrosomal CEP152 level decreased with entering mitosis and increased by Plk1 inhibition in my observation. Because of these quite interesting behaviors of CEP152, my fundamental two questions are (1) how the centromal levels are reduced and (2) how Plk1 regulates the centrosomal levels of CEP152. Even though these questions are questions about the regulatory mechanisms mainly at prometaphase, I believed that this CEP152 regulation by Plk1 would be related to centriole-to-centrosome in early G1 phase, because this Plk1 which is essential for the conversion mechanisms and CEP152 is the one of conversion factors.

From my experiments, I've obtained important facts to establish a model of regulatory mechanisms on CEP152 in mitosis. First, a domain necessary for centrosomal localization changes with cell's entering mitosis. Second, an interaction between CEP152 and CEP63 is strong and essential for centrosomal localization throughout cell cycle. Third,

interactions of CEP152 with either CEP295 or CPAP is getting weaker in mitosis. Forth, inhibition of Plk1 or depletion of CEP192 made centrosomal CEP152 level higher in mitosis, which alludes that Plk1 activation and the presence of CEP192 reduce centrosomal CEP152 level in mitosis.

In previous studies about the interaction domain of CEP152, it has been revealed that CEP152's 1205-1272aa region (out of 1-1654aa) interacts with CEP63 (Kim et al., 2019b). This region is in my CEP152 #5 fragment (1045-1289aa) of which region is crucial for centrosomal localization in interphase. On top of that, CEP152's 784-1654aa region is interacts with CPAP (Cizmecioglu et al., 2010) and Asterless/CEP152's 531-994aa (out of 1-994aa) interacts with Ana1/CEP295 in drosophila cell (Fu et al., 2016). These regions of CEP152 and Asterless is like a region in my CEP152 #4+5+6 fragment (749-1654aa) of which region is important for centrosomal localization in mitosis and centrosomal level increment with BI2536 or siCEP192 treatment. Thus, it is most likely that interaction of CEP152-CEP63 is a main reason for centrosomal localization in interphase and interactions of CEP152-CEP295 and CEP152-CPAP are a reason for mitotic centrosomal localization. In fact, depletion of CEP295 or CPAP made centrosomal level lower in mitosis and BI2536 treated condition in my results which support the hypothesis that CEP295 and CPAP are interacting with CEP152 in mitosis. However, I observed strong interaction of CEP152-CEP295 and CEP152-CPAP in

interphase compare to mitosis. Also, it has been reported that CEP152 needs to interact with CEP295 and CPAP to perform proper centriole assembly activity in previous researches (Fu et al., 2016; Lattao et al., 2017). So, it seems like CEP295 and CPAP need to be interaction partners not only in mitosis, but also in interphase. Contradiction comes up from here because the interaction partner for centrosomal localization in interphase and mitosis should be different according to my experimental result. In addition, CEP152-CEP63 interaction is important for centrosomal localization through whole cell cycle, not in interphase only. If CEP152-CEP63 interaction is important for centrosomal localization only in interphase, centrosomal CEP152 level wouldn't be low in mitotic CEP63 depleted cells. The result of CEP63 depletion suggested that CEP152-CEP63 interaction is fundamental basis for centrosomal localization. Thus, another protein excluding CEP63, CEP295 and CPAP needs to exist. By adding up this CEP152's interphase partner, the contradiction can be solved clearly.

As for a candidate responsible for centrosomal localization in interphase, I believe that CEP57 has high possibility to be the candidate. Because, Chemical crosslinking experiment revealed a CEP57-CEP63-CEP152 centrosomal complex (Lukinavičius et al., 2013) and as it happens, CEP57 is a reason for PACT domain's centrosomal localization (Watanabe et al., 2019). Anyway, CEP152-CEP63 building block would be localized to centrosome first by the "Interphase partner", which might be CEP57,

and I call it as a primary centrosomal localization. After the primary localization, CEP152 would be docking to CEP295 and CPAP. This would be a reason for CEP152's interaction with CEP295 and CPAP in interphase and solve the contradiction comes from the fact that CEP295 and CPAP cannot be CEP152's interaction partners for centrosomal localization in interphase. For instance, CEP152 Δ4 and Δ6, which have #5 region, can be localized at centrosome interphase but they can't be in mitosis even with BI2536 treatment and I believe that is mainly because these mutants cannot interact with CEP295 and CPAP according to previous CEP152 interaction domain studies (Cizmecioglu et al., 2010; Fu et al., 2016). However, these mutants can be localized to centrosome in interphase most probably due to their primary centrosomal localization.

In mitosis, the minimum fragments for centrosomal level increment induced by Plk1 inhibition and centrosomal localization in mitosis are same. Therefore, I claim that Plk1 activity weakens the interaction of CEP152-CEP295 and CEP152-CPAP which leads to centrosomal level reduction in mitosis. On top of that, depletion of CEP192 has an effect as similar as Plk1 inhibition, and it has been reported that CEP192 is a platform for Plk1 and Aurora A to be activated in mitosis for centrosome maturation and bipolar spindle assembly (Joukov et al., 2014). Therefore, I insist that CEP192 activating Plk1 reduces centrosomal CEP152 level by phosphorylation which is mainly caused by weakening the interaction of CEP152-CEP295 and CEP152-

CPAP.

Then, what did happen to the interphase partner? How can the interaction between CEP152 and its interphase partner disappear and CEP152's interaction partner is shifted to CEP295 and CPAP? Does a phosphorylation by plk1 break the interphase interaction? If the phosphorylation by Plk1 is the reason for blocking the interaction in interphase, at least it must be selectively irreversible. For instance, good example is CEP152 Δ4 and Δ6 which are only able to interact with the interphase partner not CEP295 or CPAP. If the blocking mechanism on the interphase interaction is reversible, centrosomal level of these mutants would have increased by BI2536 treatment, because these mutants would have interacted with interphase partner again by plk1 inhibition. Since the blocking mechanism is either a selectively irreversible mechanism regulated by plk1 or regulated by another reason, Plk1 inhibition didn't make centrosomal level of CEP152 Δ4 and Δ6 higher.

For some reason, CEP152 shifts its interaction partner to CEP295 and CPAP with cell's entering mitosis and the interaction is reduced by Plk1 activity. This Plk1 is activated in late G2 phase (Gheghiani et al., 2017) and Plk1 is inactivated by degradation in anaphase (Lindon and Pines, 2004), although, centriole-to-centrosome conversion occurs after exiting mitosis. In addition, CEP152's scaffold CEP295 is already localized at

daughter centriole in late mitosis (Tsuchiya et al., 2016). Then, what does block the centrosomal localization of CEP152 to the daughter centriole, ready to be a mother centriole, until exiting mitosis? Recent study in our lab has revealed that pericentrin cleavage is necessary for converting centriole to recruit CEP152 (Kim et al., 2019a), and this cleavage of pericentrin induces disintegration of PCM. Thus, I think that this pericentrin might be an interaction breaker for CEP152 and CEP57, if CEP57 is an interphase interaction partner of CEP152-CEP63 building block.

As already mentioned, CEP57 is the protein interacting with a PACT domain and pericentrin has the PACT domain. When centrosome maturation occurs, which is also regulated by Plk1 (Kim and Rhee, 2014), pericentrin is recruited to the PCM a lot and it would snatch the CEP57 from CEP152-CEP63 probably because PACT's binding affinity to CEP57 is stronger than CEP152-CEP63's. This snatching concept was also proposed in model of CEP152 snatching Plk4 from CEP192 (Park et al., 2014). Due to the interaction between pericentrin and CEP57, CEP152-CEP63 lose its interphase interaction partner and shift its partner to CEP295 and CPAP. But these interactions are weakened by Plk1 with entering mitosis, so centrosomal CEP152 level decreases. In late mitosis, Plk1 is degraded and CEP295 exists, but CEP152 cannot be localize at converting centriole because pericentrin is still interacting with CEP57 strongly until the pericentrin is cleaved by separase. And I suggest this

hypothesis as a regulatory mechanism for centrosomal CEP152 with cell's entering and exiting mitosis.

Since I didn't reveal an interphase interaction partner of CEP152, I propose my model for centrosomal CEP152 regulation in mitosis only with the results I found (Fig. 28). Interaction between CEP63 and CEP152 is strong in interphase and mitosis, and this interaction is not inhibited by Plk1 activity. Centrosomal CEP152 level reduces with entering mitosis, because of the Plk1 kinase activated by CEP192 working as a platform. Phosphorylation by the plk1 weakens the CEP152 interactions with CEP295 and CPAP.

The concept of primary centrosomal localization by an interphase interaction partner of CEP152 and the other concept, the shifting of domain important for centrosomal localization don't appear in my model due to an absence of experimental results. However, I strongly believe that there must be another key protein interacting with CEP152 especially in interphase. Since CEP152 is well known for a conversion factor in G1 phase and centriole assembly function from S phase, most of researches about CEP152 have been mainly focusing on cell cycle after exiting mitosis. Also, direct regulation of centrosomal CEP152 level by Plk1 hasn't been reported. In this perspective, my research has a novelty because most of my observations were carried out with entering mitosis and I found out that Plk1 regulates protein-protein interactions between

CEP152 and its interaction candidates which affected centrosomal CEP152 localization. Furthermore, crucial clues were obtained by my research for connecting the centrosomal CEP152 level regulation by plk1 with centriole-to-centrosome conversion mechanism. I believe that further studies started from my research will elucidate the uncertain mechanisms of conversion.

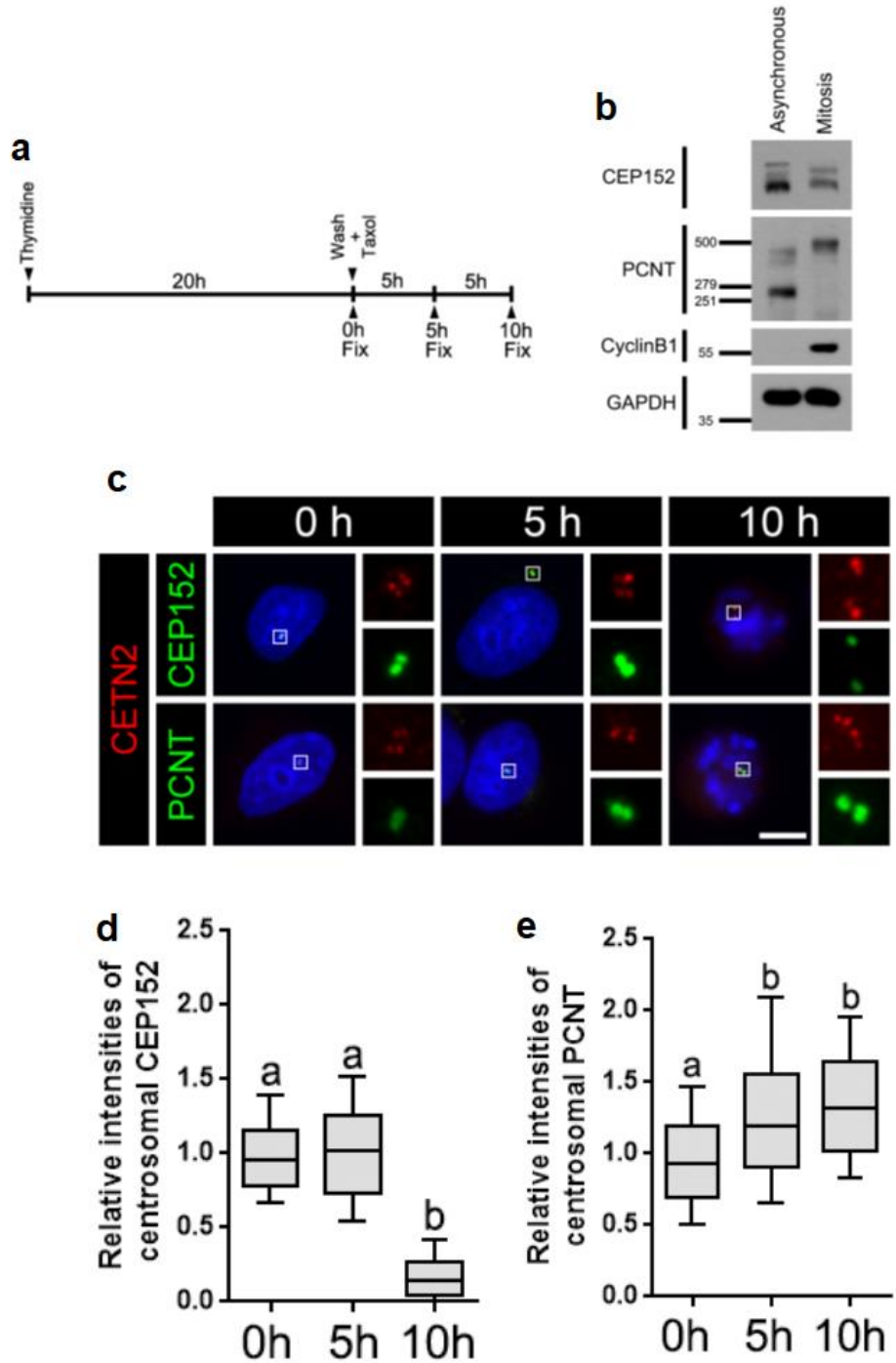

Figure 6. Reduction of the centrosomal CEP152 levels at the onset of mitosis

Figure 6. Reduction of the centrosomal CEP152 levels at the onset of mitosis (**a**) HeLa cells were treated with thymidine for 20 h and sequentially treated with paclitaxel (Taxol). The cells were harvested at indicated time points (0h, 5h and 10h) and subjected to immunostaining analyses. (**b**) Most of cells in the 10h group were arrested at prometaphase. Immunoblot analysis were carried out with antibodies specific to CEP152, PCNT, cyclin B1 and GAPDH. (**c**) The cells were coimmunostained with the centrin-2 antibody (CETN2, red), along with the CEP152 and pericentrin (PCNT) antibodies (green). DNA was visualized with DAPI (blue) and the mitotic stages were determined with DAPI staining patterns. Scale bar, 10 μm. (**d-e**) Centrosomal intensities of the CEP152 (**d**) and PCNT (**e**) signals were shown with the box-and-whisker plot. n=120 per group in 2 independent experiments. The statistical significance was determined by one-way ANOVA and Turkey's multiple comparisons test in Prism 6 and was indicated by lower cases ($P<0.0001$).

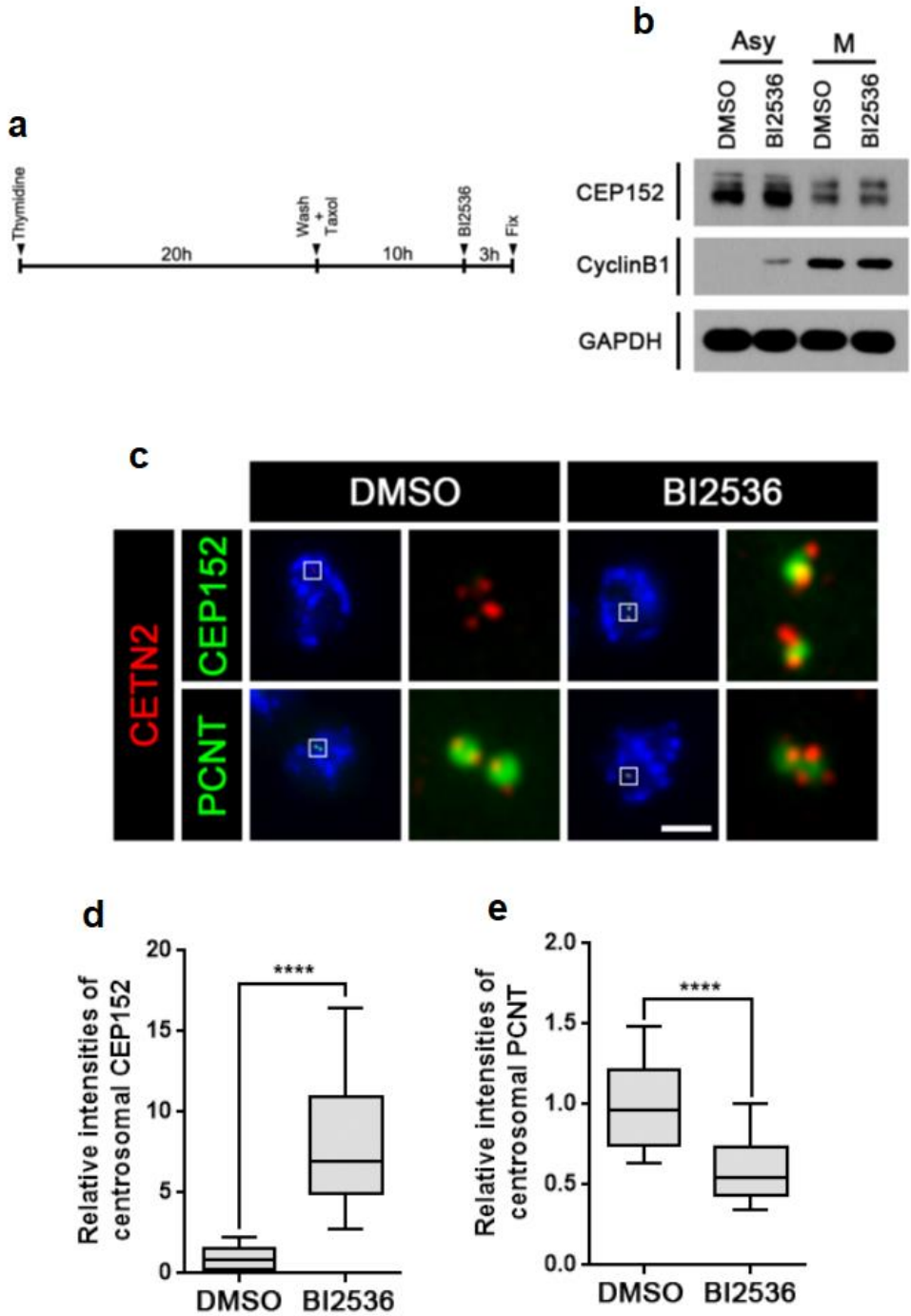

Figure 7. Effects of BI2536 on CEP152 levels in the centrosomes of mitotic cells

Figure 7. Effects of BI2536 on CEP152 levels in the centrosomes of mitotic cells (**a**) HeLa cells were arrested at M phase with sequential treatment of thymidine and Taxol. BI2536 was added for the last 3 h for Plk1 inhibition. (**b**) Mitotic HeLa cells (M) were harvested with or without BI2536 treatment for 3 h. Asynchronous HeLa cells (Asy) were harvested with the same scheme of mitotic sample without thymidine and Taxol. The cells were subjected to immunoblot analysis with antibodies specific to CEP152, cyclin B1 and GAPDH. (**c**) The cells were coimmunostained with the centrin-2 antibody (CETN2, red), along with the CEP152 and pericentrin (PCNT) antibodies (green). DNA was visualized with DAPI (blue) and the mitotic stages were determined with DAPI staining patterns. Scale bar, 10 μm. (**d-e**) Centrosomal intensities of the CEP152 (**d**) and PCNT (**e**) signals were shown with the box-and-whisker plot. n=180 per group in 3 independent experiments. The statistical significance was determined by unpaired t test in Prism 6 (****, $P<0.0001$).

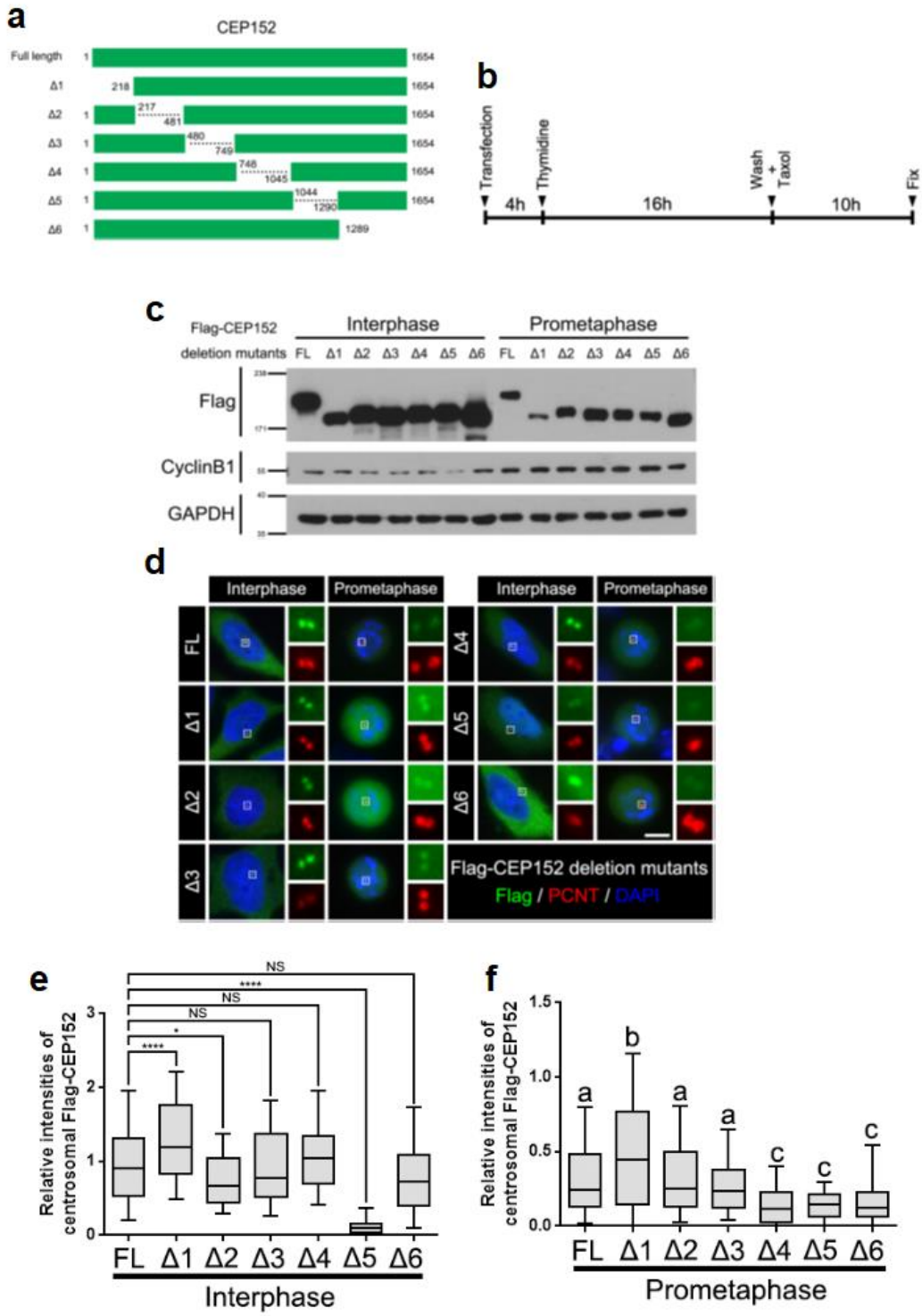

Figure 8. Centrosomal levels of the CEP152-truncated mutants in mitosis

Figure 8. Centrosomal levels of the CEP152-truncated mutants in mitosis (**a**) A serial truncated mutants of CEP152 were generated (Δ1~Δ6). A Flag tag was attached at the N-terminal ends of the truncated mutants. (**b**) HeLa cells were arrested at M phase with sequential treatment of thymidine and TaxoI after DNA transfection. (**c**) The cells at prometaphase subjected to Immunoblot analyses with antibodies specific to CEP152, cyclin B1 and GAPDH. (**d**) The cells were coimmunostained with the Flag (green) and pericentrin (PCNT, red) antibodies. DNA was visualized with DAPI (blue). Scale bar, 10 μm. (**e-f**) Centrosomal intensities of the Flag-CEP152 signals in Interphase (**e**) and mitosis (**f**) were shown with the box-and-whisker plot. n=120 per group in 2 independent experiments. The statistical significance was determined by one-way ANOVA and Turkey's multiple comparisons test in Prism 6 (NS, $P>0.05$; *, $P<0.05$; ****, $P<0.0001$) and was indicated by lower cases ($P<0.5$).

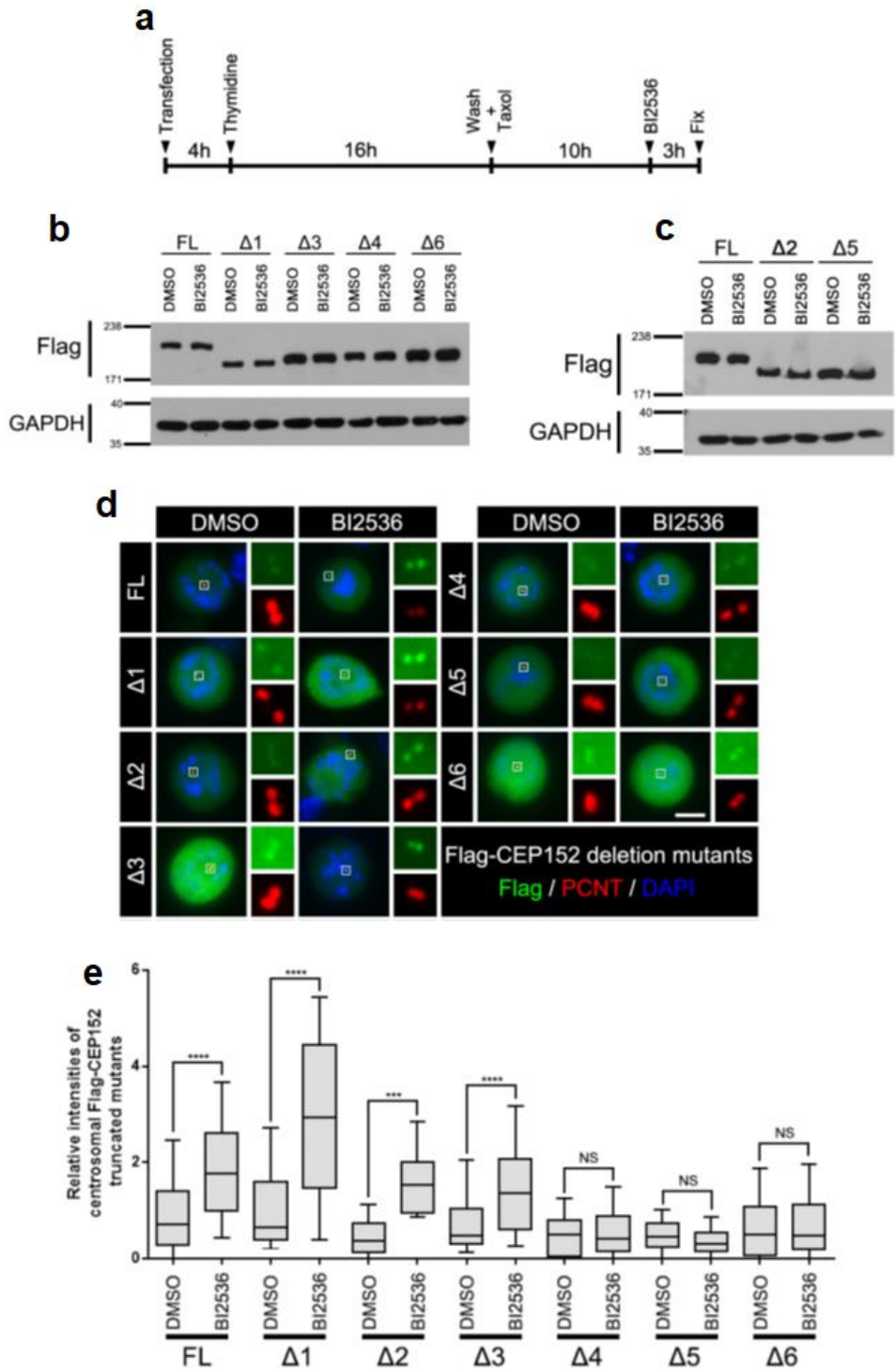

Figure 9. Effects of BI2536 on centrosomal levels of the CEP152-truncated mutants

Figure 9. Effects of BI2536 on centrosomal levels of the CEP152-truncated mutants
(**a**) HeLa cells were arrested at M phase with sequential treatment of thymidine and Taxol after DNA transfection. BI2536 was added for the last 3 h for Plk1 inhibition. (**b-c**) HeLa cells were harvested with or without BI2536 treatment for 3 h. Ectopic Flag-CEP152 Full length (FL), Δ1, Δ3, Δ4 and Δ6 were detected by immunoblot analysis using Flag and GAPDH antibodies (**b**), and ectopic Flag-CEP152 Full length (FL), Δ2, Δ 5 were detected with same analysis (**c**). (**d**) The cells were fixed and coimmunostained with Flag (green) and pericentrin (PCNT, red) antibodies. DNA was visualized with DAPI (blue). Scale bar, 10 μm. (**e**) Centrosomal intensities of the Flag-CEP152-truncated mutants signals with or without BI2536 treatment were shown with the box-and-whisker plot. n=120 per group in 2 independent experiments. The statistical significance was determined by one-way ANOVA and Turkey's multiple comparisons test in Prism 6 (NS, $P>0.05$; ***, $P<0.001$; ****, $P<0.0001$).

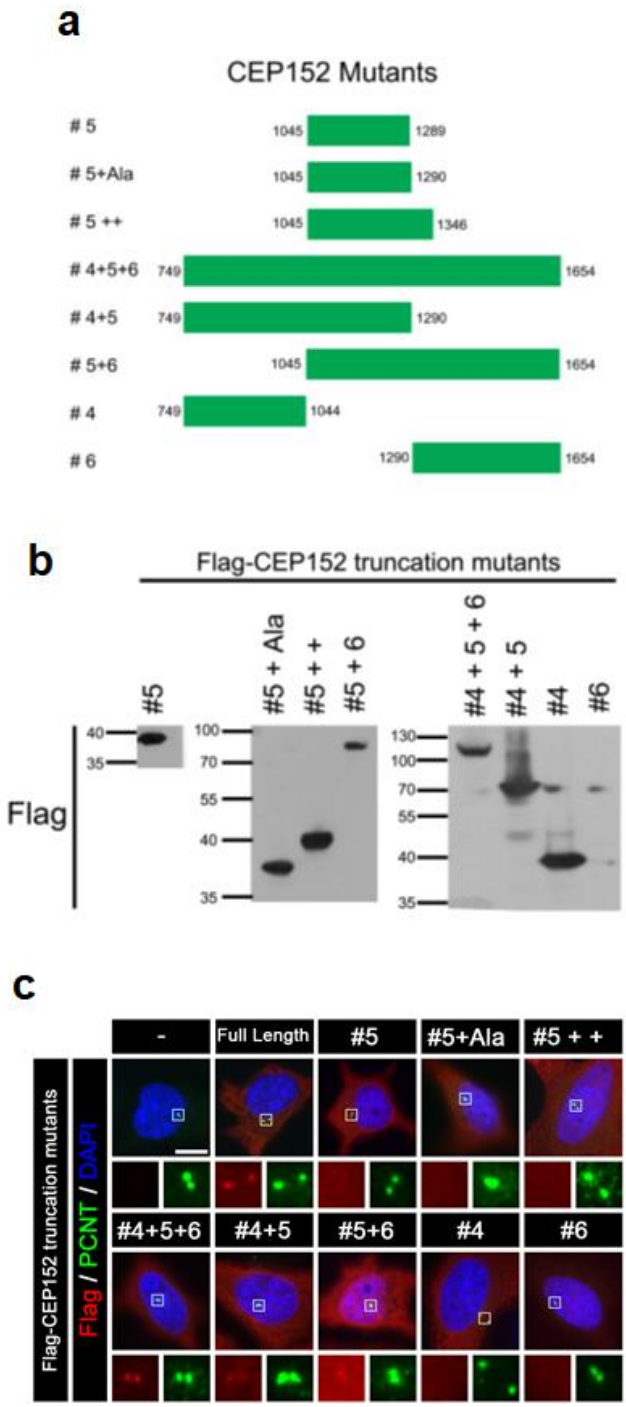

Figure 10. Centrosomal levels of of the Flag-CEP152 deletion fragments in mitotic cells

Figure 10. Centrosomal levels of of the Flag-CEP152 deletion fragments in mitotic cells (**a**) Various ectopic Flag-CEP152 deletion fragments were generated. (**b**) HeLa cells were harvested in 24 h after DNA transfection of the ectopic CEP152 deletion fragments and subjected to immunoblot analysis with antibodies specific to Flag. (**c**) HeLa cells were fixed in 24 h after DNA transfection and coimmunostained with the Flag (red) and pericentrin (PCNT, green) antibodies. DNA was visualized with DAPI (blue). Scale bar, 10 μm.

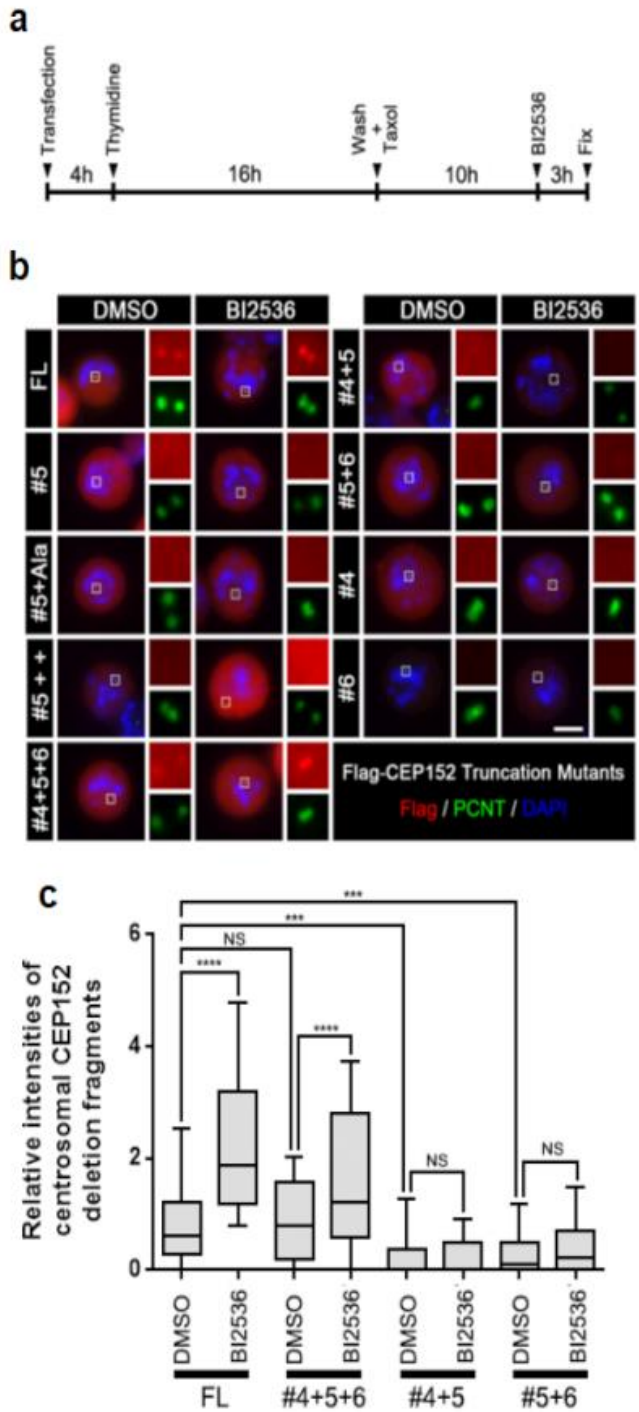

Figure 11. Effects of BI2536 on centrosomal levels of the Flag-CEP152 deletion fragments at prometaphase

Figure 11. Effects of BI2536 on centrosomal levels of the Flag-CEP152 deletion fragments at prometaphase (**a**) HeLa cells were arrested at M phase with sequential treatment of thymidine and Taxol after DNA transfection. BI2536 was added for the last 3 h for Plk1 inhibition. (**b**) Cells were fixed and coimmunostained with Flag (red) and pericentrin (PCNT, green) antibodies. DNA was visualized with DAPI (blue). Scale bar, 10 μm. (**c**) Centrosomal intensities of the Flag-CEP152 deletion fragments signals with or without BI2536 treatment were shown with the box-and-whisker plot. n=120 per group in 2 independent experiments. The statistical significance was determined by one-way ANOVA and Turkey's multiple comparisons test in Prism 6 (NS, $P>0.05$; ***, $P<0.001$; ****, $P<0.0001$).

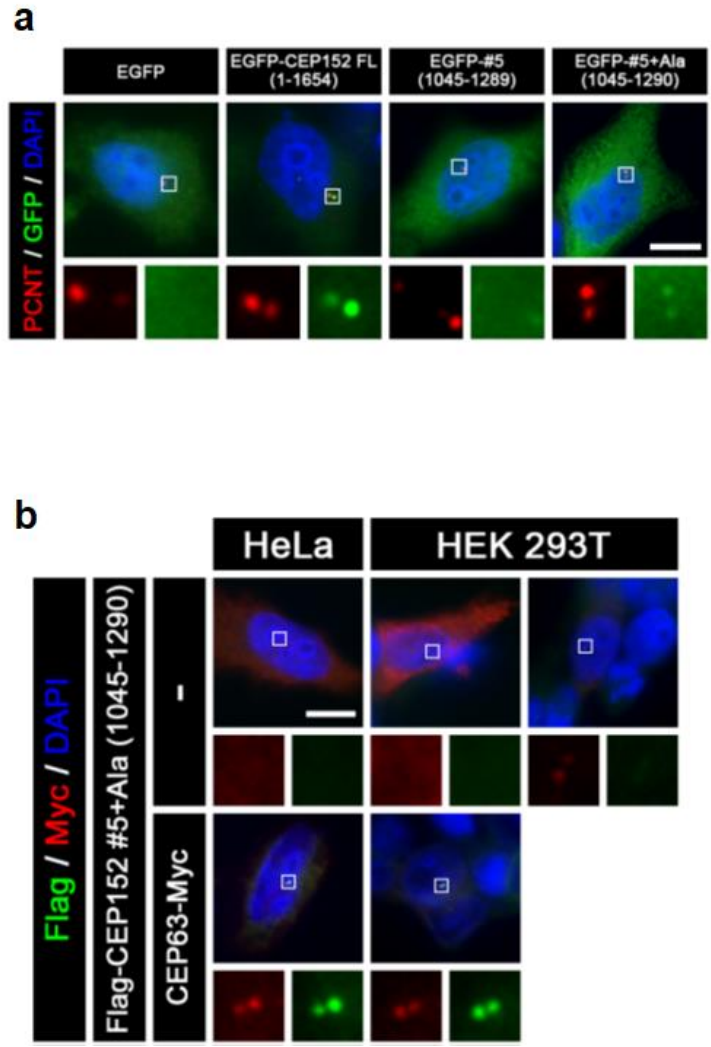

Figure 12. Determination of CEP152 fragments important for centrosomal localization (**a**) HeLa cells were fixed in 24 h after DNA transfection and coimmunostained with antibodies specific to pericentrin (PCNT, red) and GFP (green). DNA was visualized with DAPI (blue). Scale bar, 10 μm. (**b**) coimmunostaining analysis of HeLa cells and HEK 293 T cells 24 h after DNA transfection with a single Flag-CEP152 fragment or a mixture of CEP63-Myc and Flag-CEP152 fragment. Antibodies specific to Flag (green) and Myc (red) were used. Scale bar, 10 μm.

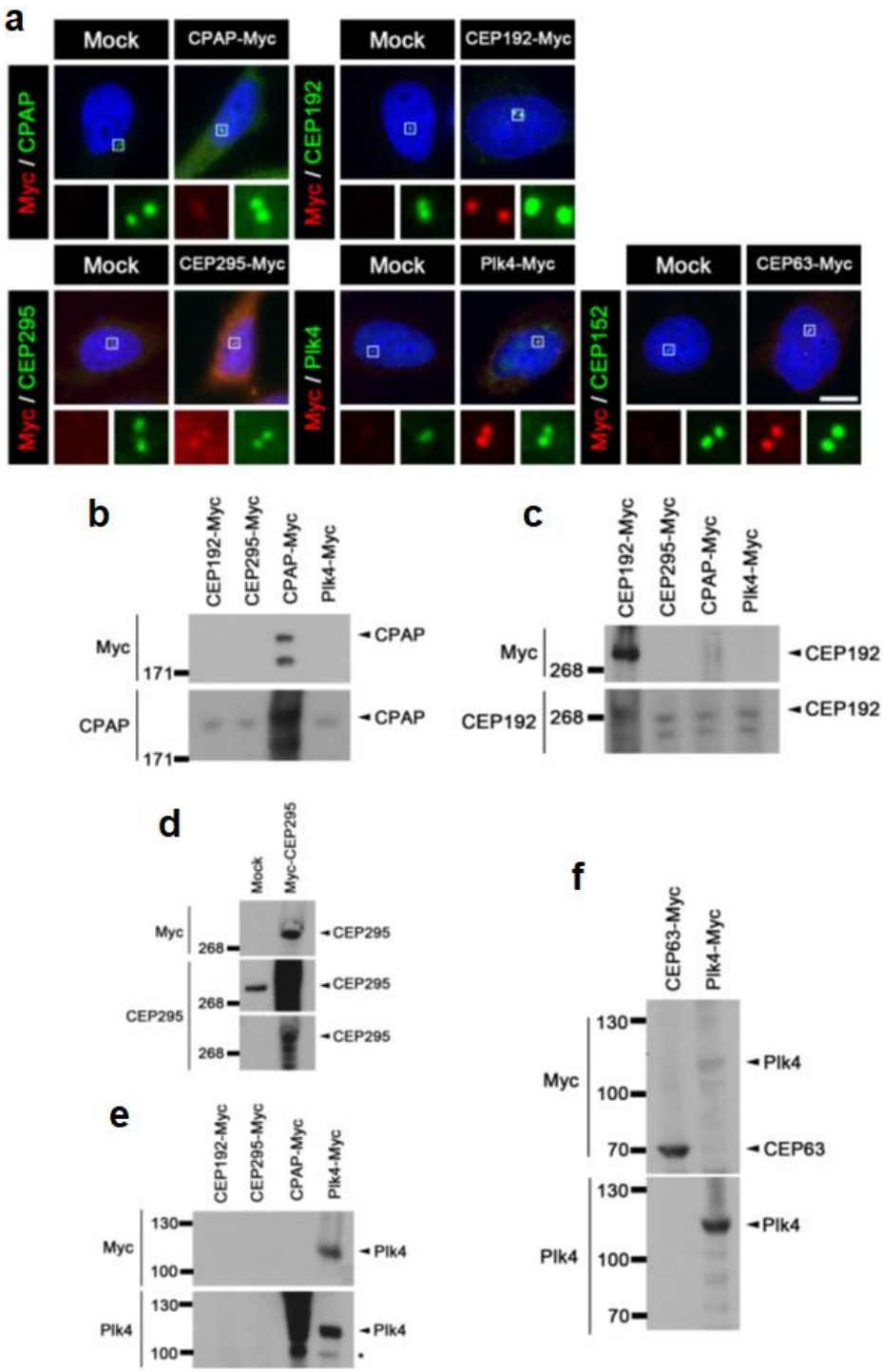

Figure 13. Ectopic expression of the candidate CEP152-interaction proteins

Figure 13. Ectopic expression of the candidate CEP152-interaction proteins (**a**) HeLa cells were fixed in 24 h after DNA transfection with indicated constructs and coimmunostaining analysis was carried out with indicated antibodies (Myc, red). DNA was visualized with DAPI (blue). Scale bar, 10 μm. (**b**-**f**) HEK 293T cells were harvested 24 h after DNA transfection with indicated constructs and immunoblot analysis were carried out to check expression of the ectopic CPAP (**b**), CEP192 (**c**), CEP295 (**d**), Plk4 (**e**) and CEP63 (**f**). Antibodies specific to Myc, CPAP, CEP192, CEP295 and Plk4 were used to detect endogenous proteins and ectopic proteins with a Myc tag. Due to unavailability of CEP63 antibody, only Myc antibody was used to detect the ectopic CEP63-Myc construct.

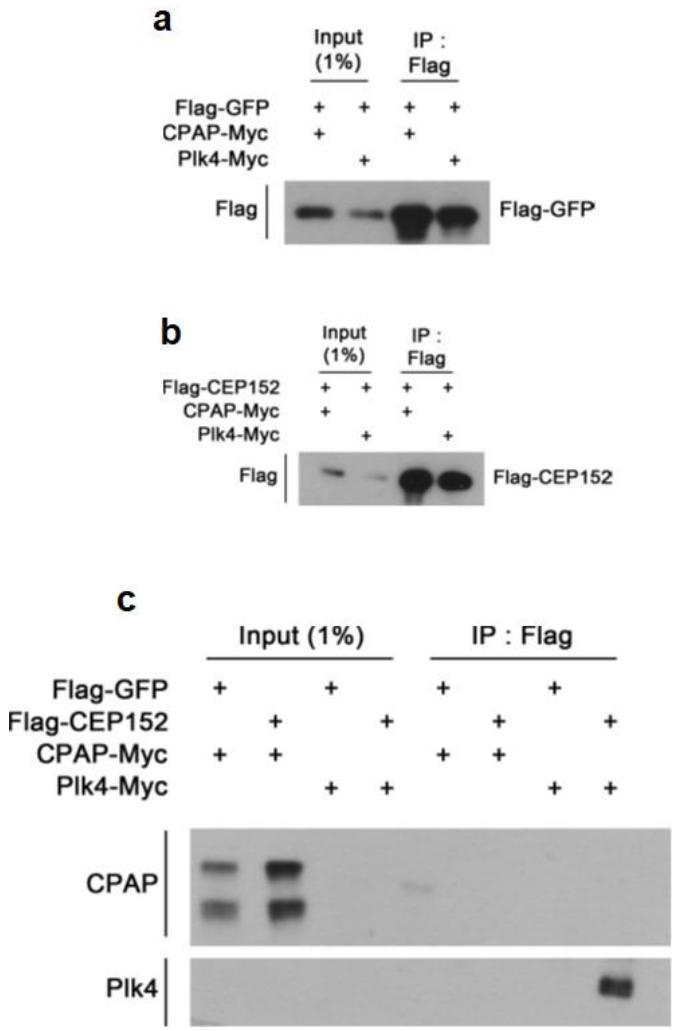

Figure 14. Co-immunoprecipitation of the ectopic Plk4 and CPAP with the Flag-CEP152 (**a-c**) HEK 293T cells were harvested and immunoprecipitated by the anti-FLAG M2 Agarose Beads in 24 h after DNA transfection with indicated constructs. Immunoblot analysis were carried out with antibodies specific to Flag, CPAP and Plk4. Flag-GFP was used as a control construct for the Flag-CEP152 construct. The Flag-GFP (**a**) and the Flag-CEP152 (**b**) were immunoprecipitated. (**c**) Plk4 was co-immunoprecipitated only with the Flag-CEP152. Co-immunoprecipitated CPAP was not detected for this immunoblot analysis.

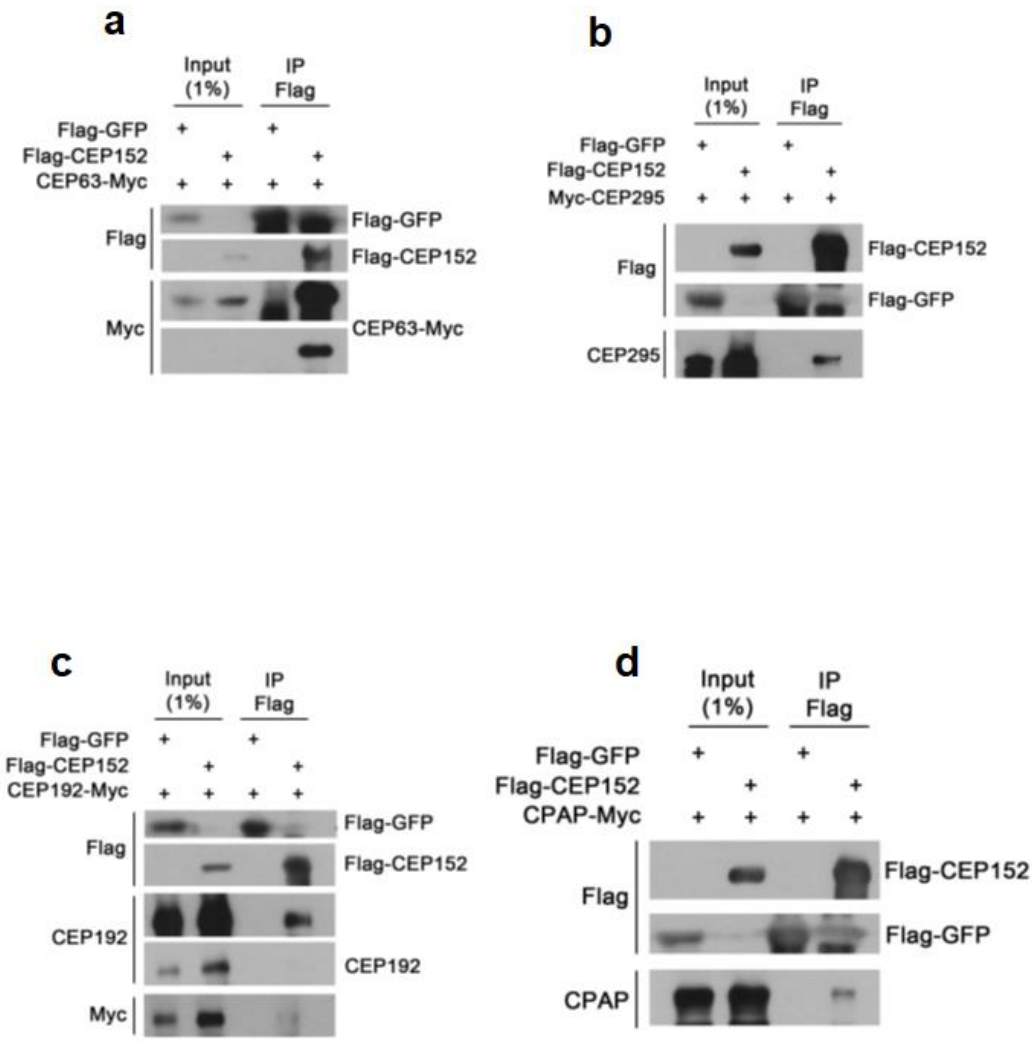

Figure 15. Co-immunoprecipitation of the ectopic CEP63, CEP295, CEP192 and CPAP with the Flag-CEP152 (**a-d**) HEK 293T cells were harvested and immunoprecipitated by the anti-FLAG M2 Agarose Beads in 24 h after DNA transfection with indicated constructs. Immunoblot analysis were carried out with antibodies specific to Flag, Myc, CEP295, CEP192 and CPAP. Flag-GFP was used as a control construct for the Flag-CEP152. All target proteins were co-immunoprecipitated inly with the Flag-CEP152. (**a**) : CEP63, (**b**) : CEP295, (**c**) : CEP192, (**d**) : CPAP.

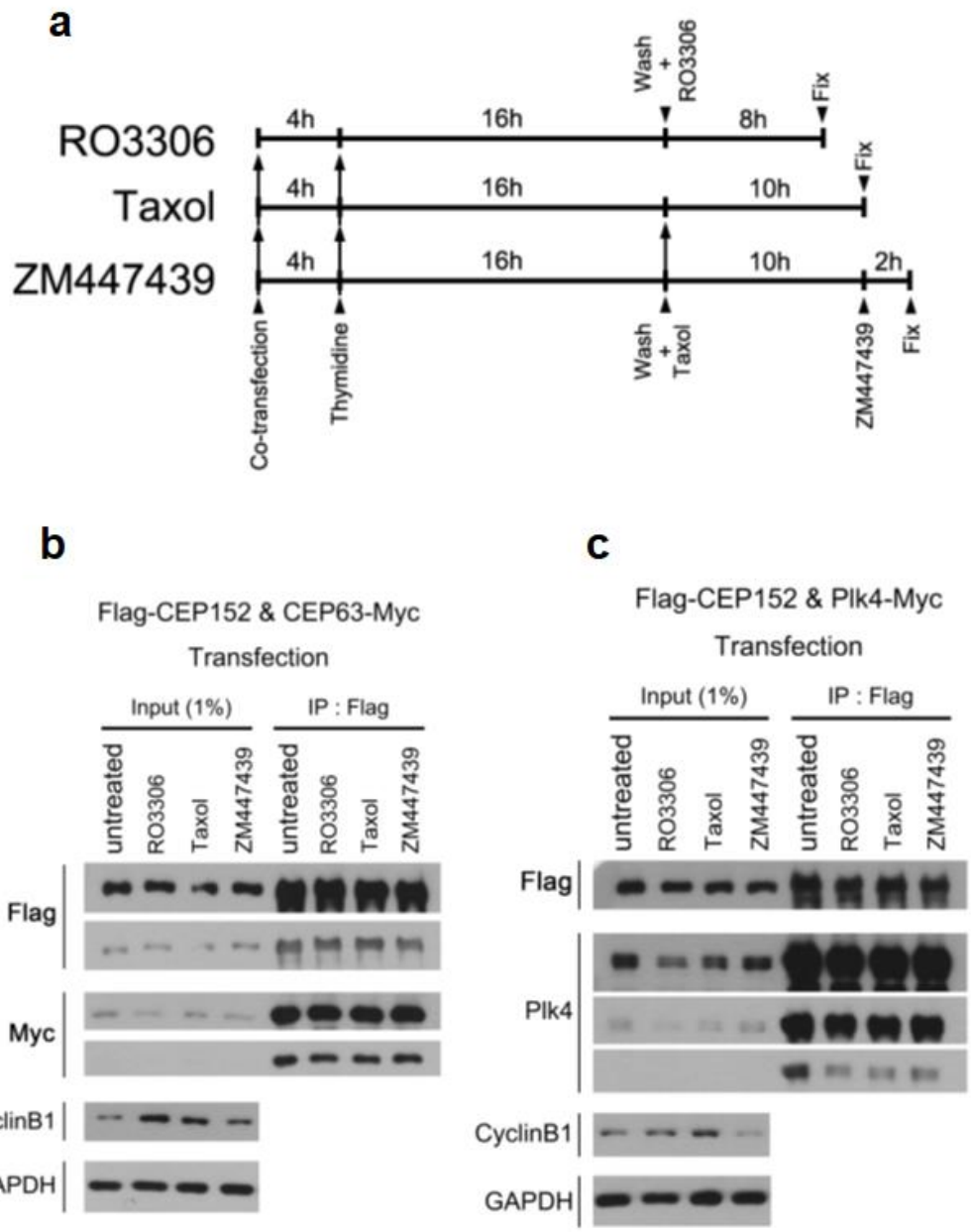

Figure 16. Effects of the cell cycle blocking drugs on Flag-CEP152 interaction with ectopic CEP63 and Plk4

Figure 16. Effects of the cell cycle blocking drugs on Flag-CEP152 interaction with ectopic CEP63 and Plk4 (**a**) HEK 293T cells were arrested at different cell cycle points. Cells were supposed to be arrested at late G2 phase by sequential treatment of thymidine and RO3306, prometaphase by sequential treatment of thymidine and Taxol and early G1 phase by treating ZM447439 for 3 h on prometaphase arrested cells. Arrested cells were harvested and immunoprecipitated by the anti-FLAG M2 Agarose Bead at indicated 'Fix' time point. (**b-c**) Immunoblot analysis was carried out to determine the amount of co-immunoprecipitated CEP63 (**b**) or Plk4 (**c**) by the Flag-CEP152 for untreated group, RO3306 group, Taxol group and ZM447439 groupwith indicated antibodies on the left side of figure.

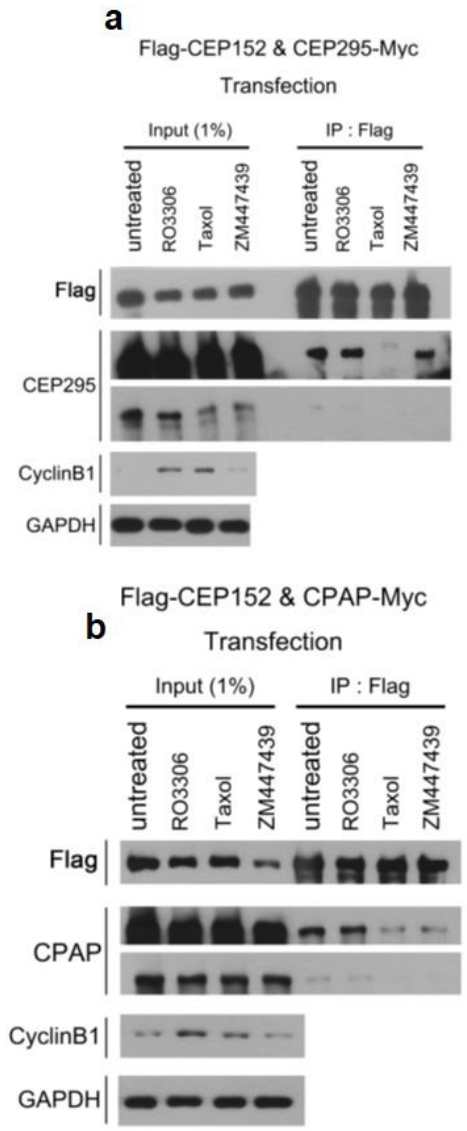

Figure 17. Effects of the cell cycle blocking drugs on Flag-CEP152 interaction with ectopic CEP295 and CPAP (**a**-**b**) Immunoblot analysis was carried out to determine the amount of co-immunoprecipitated CEP295 (**a**) or CPAP (**b**) by the Flag-CEP152 for untreated group, RO3306 group, Taxol group and ZM447439 group with indicated antibodies on the left side of figure.

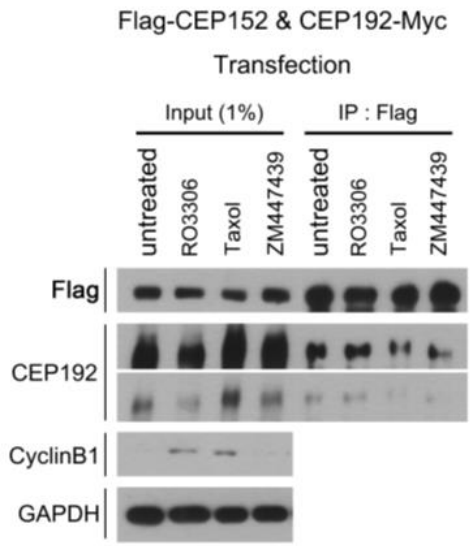

Figure 18. Effects of the cell cycle blocking drugs on Flag-CEP152 interaction with ectopic CEP192 Immunoblot analysis was carried out to determine the amount of co-immunoprecipitated CEP192 by the Flag-CEP152 for untreated group, RO3306 group, Taxol group and ZM447439 groupwith indicated antibodies on the left side of figure.

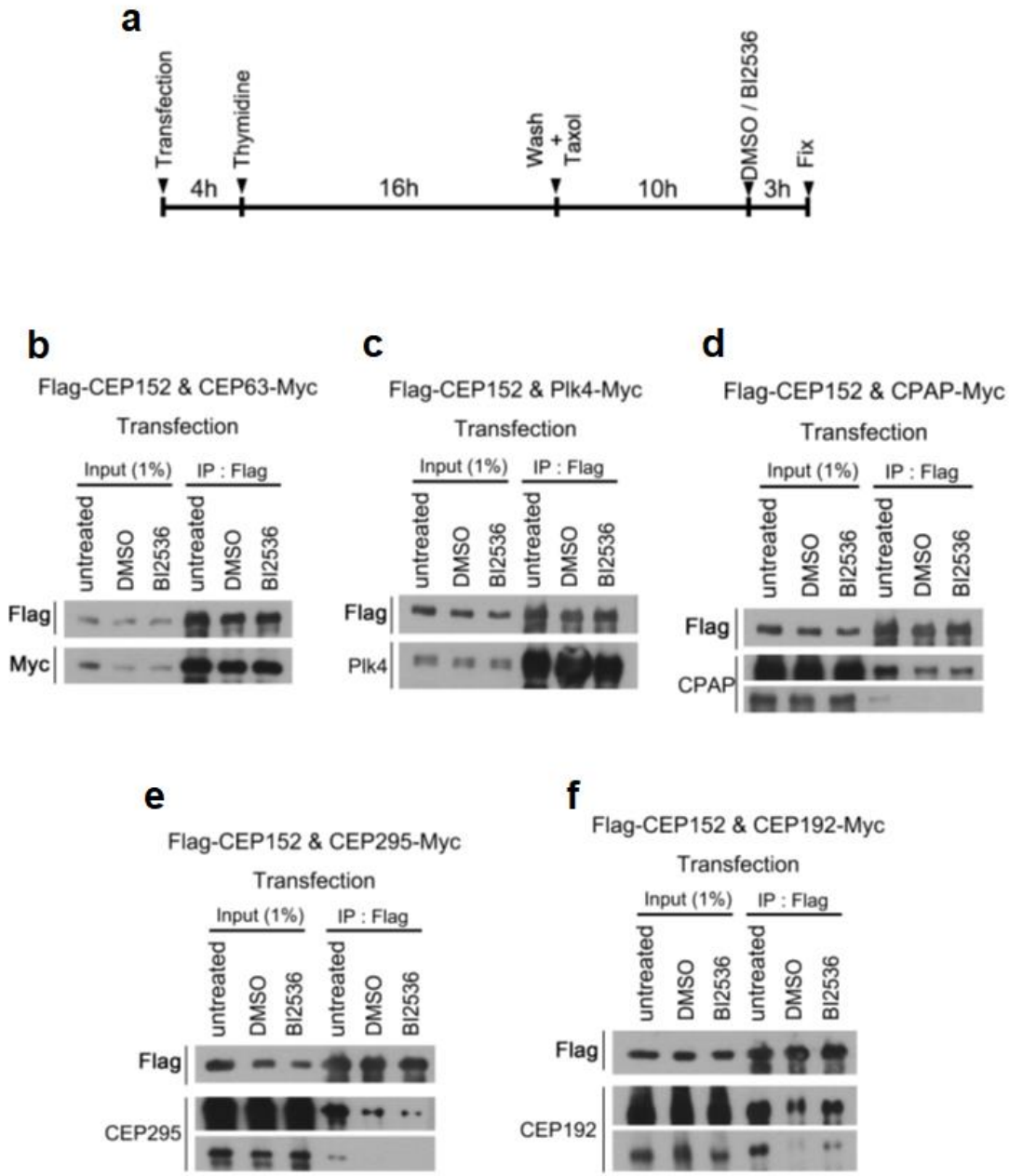

Figure 19. Effects of BI2536 on CEP152 interaction with ectopic candidate proteins

Figure 19. Effects of BI2536 on CEP152 interaction with ectopic candidate proteins
(**a**) HEK 293T cells were arrested at M phase with sequential treatment of thymidine and Taxol after DNA transfection. BI2536 was added for the last 3 h for Plk1 inhibition. (**b-f**) Three types of HEK 293T cells were used for this immunoblot analysis. No drugs were treated on untreated group and DMSO was treated as a control drug of BI2536 on DMSO group. All 293T groups were harvested at the same time point and immunoprecipitated by the anti-FLAG M2 Agarose Bead. Immunoblot analysis was carried out to determine the amount of co-immunoprecipitated CEP63 (**b**), Plk4 (**c**), CPAP (**d**), CEP295 (**e**) and CEP192 (**f**) by the Flag-CEP152 in every group.

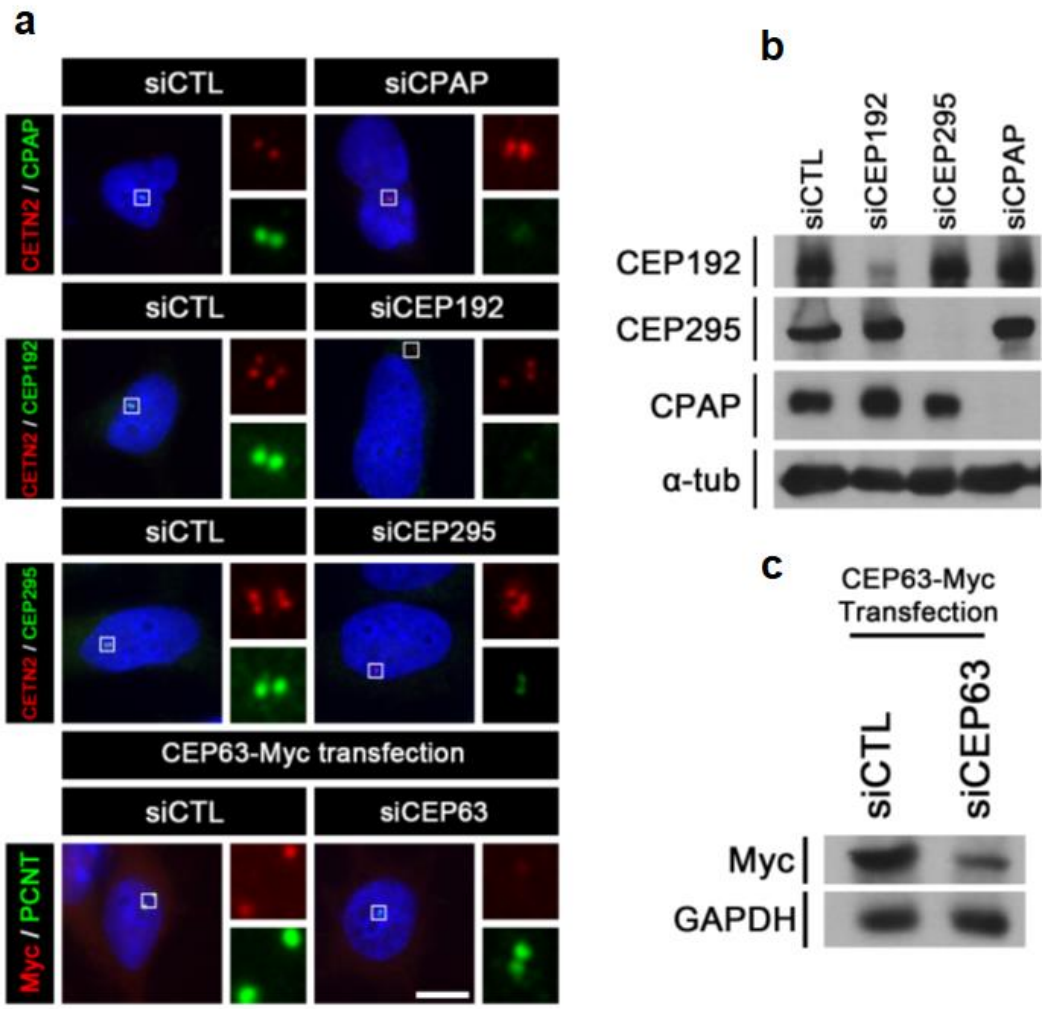

Figure 20. Depletion of CEP192, CEP295, CPAP and CEP63 with specific siRNAs (**a-c**) HeLa cells were treated each indicated siRNA for 48 h and fixed for coimmunostaining analyses (**a**) and Immunoblot analyses (**b-c**) with indicated antibodies on the left side of every figure. Due to unavailability of CEP63 antibody, knockdown efficiency of CEP63 was tested with the CEP63-Myc transfection. DNA transfection was performed in 4 h after siRNA treatment. Scale bar, 10 μm.

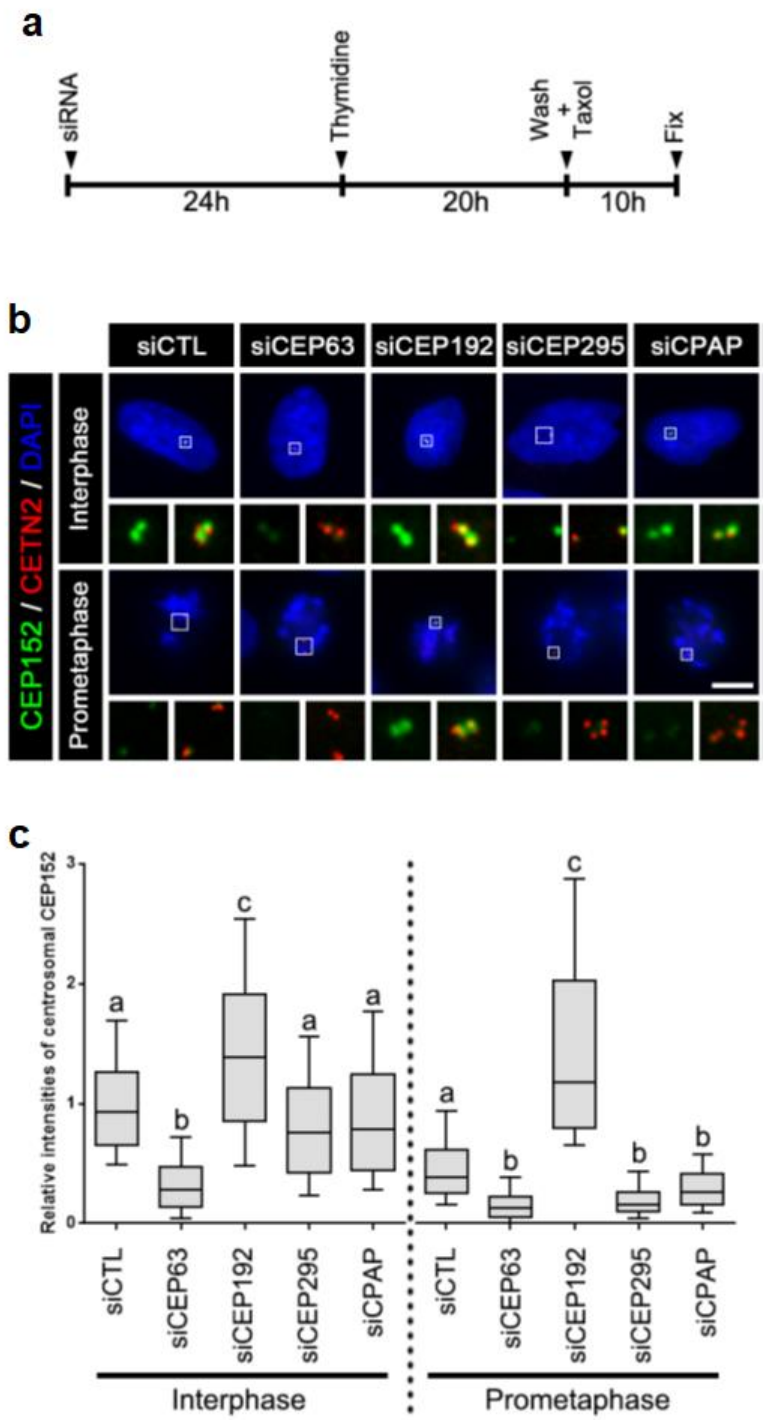

Figure 21. Centrosomal CEP152 levels in cells depleted of the CEP152-interacting proteins

Figure 21. Centrosomal CEP152 levels in cells depleted of the CEP152-interacting proteins (**a**) HeLa cells were arrested at M phase with sequential treatment of thymidine and Taxol following siRNA treatment. (**b**) The cells were fixed and analyzed by coimmunostaining with antibodies specific to CEP152 (green) and centrin-2 (CETN2, red). DNA was visualized with DAPI (blue). Scale bar, 10 μm. (**c**) Centrosomal intensities of the endogenous CEP152 signals in Interphase and mitosis were shown with the box-and-whisker plot. n=180 per group in 3 independent experiments. The statistical significance was determined by one-way ANOVA and Turkey's multiple comparisons test in Prism 6 and was indicated by lower cases ($P<0.01$).

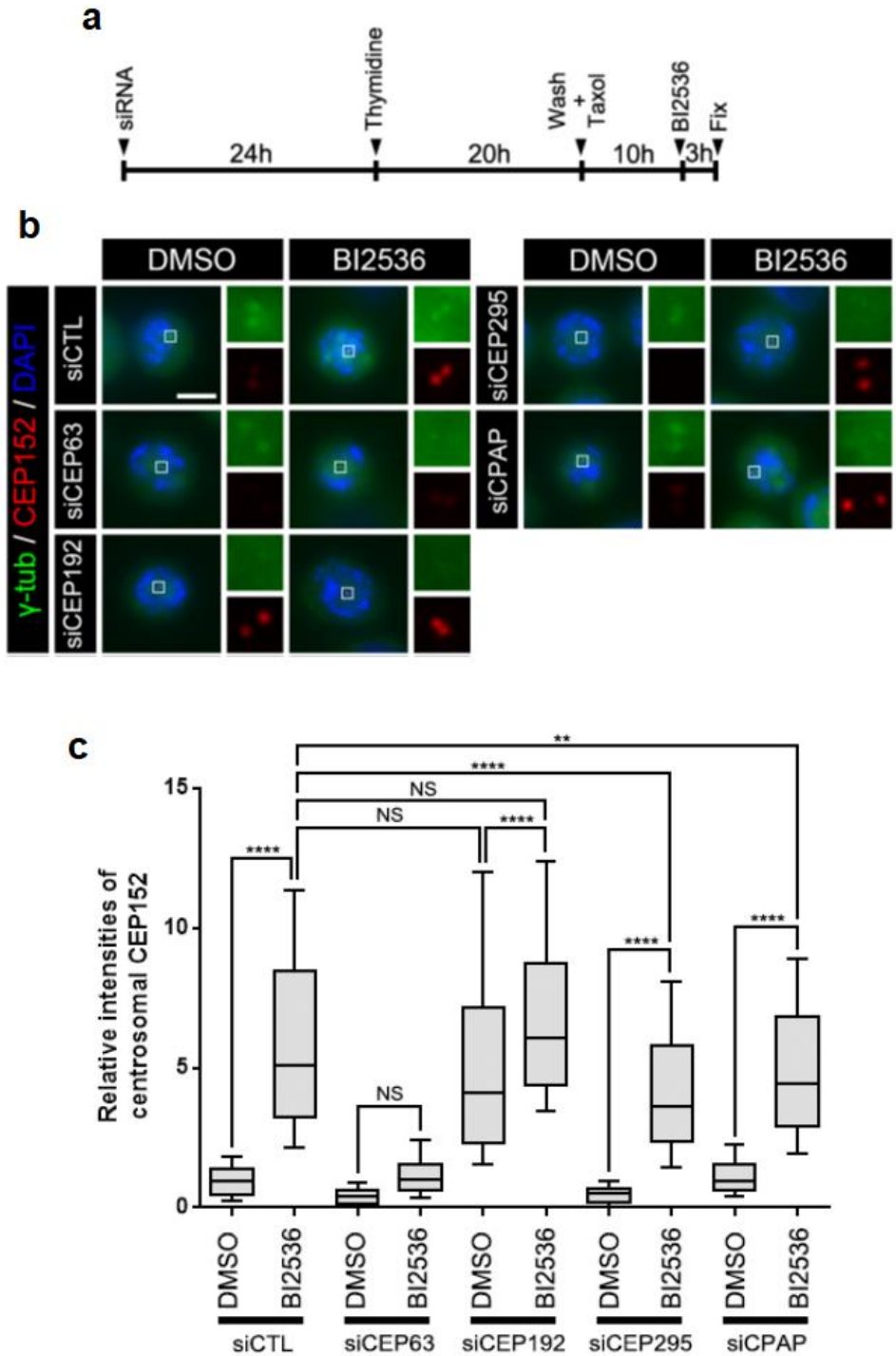

Figure 22. Effects of BI2536 on the centrosomal CEP152 levels in cells depleted of the CEP152-interacting proteins

Figure 22. Effects of BI2536 on the centrosomal CEP152 levels in cells depleted of the CEP152-interacting proteins (**a**) HeLa cells were arrested at M phase with sequential treatment of thymidine and Taxol after siRNA treatment. BI2536 was added for the last 3 h for Plk1 inhibition. (**b**) Cells were fixed and coimmunostained with γ-tubulin (green) and CEP152 (red) antibodies. DNA was visualized with DAPI (blue). Scale bar, 10 μm. (**c**) Centrosomal intensities of the endogenous CEP152 signals with or without BI2536 treatment were shown with the box-and-whisker plot. n=120 per group in 2 independent experiments. The statistical significance was determined by one-way ANOVA and Sidak's multiple comparisons test in Prism 6 (NS, $P>0.05$; **, $P<0.001$; ****, $P<0.0001$).

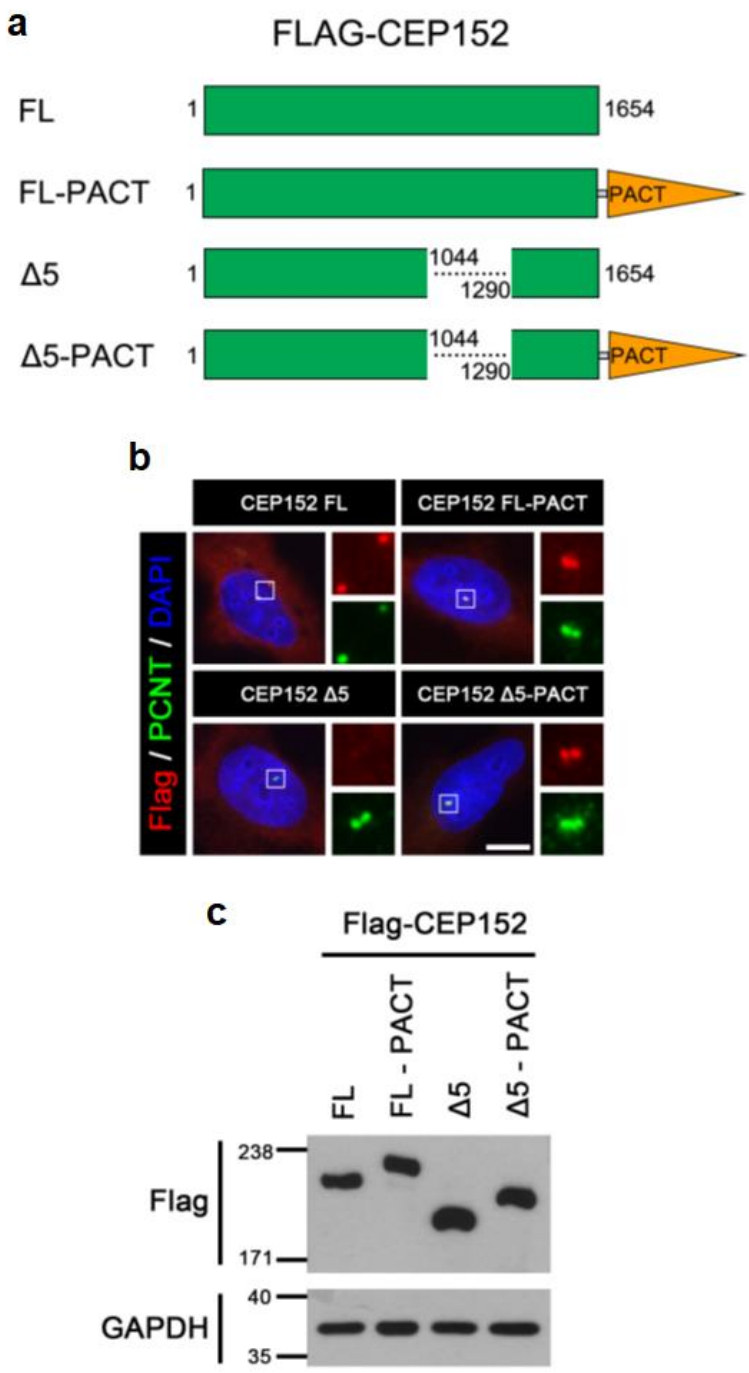

Figure 23. Centrosomal localization of the truncated Flag-CEP152-PACT proteins

Figure 23. Centrosomal localization of the truncated Flag-CEP152-PACT proteins (**a**) Pericentrin's PACT domain was fused to CEP152 Full length (FL) and CEP152 Δ5 constructs. (**b**) HeLa cells were transiently transfected with the four types of Flag-CEP152 PACT proteins. Then the cells were fixed for coimmunostaining analysis with antibodies specific to Flag (red), pericentrin (PCNT, green). DNA was visualized with DAPI (blue). Scale bar, 10 μm. (**c**) Immunoblot analysis was performed with the Flag and GAPDH antibodies.

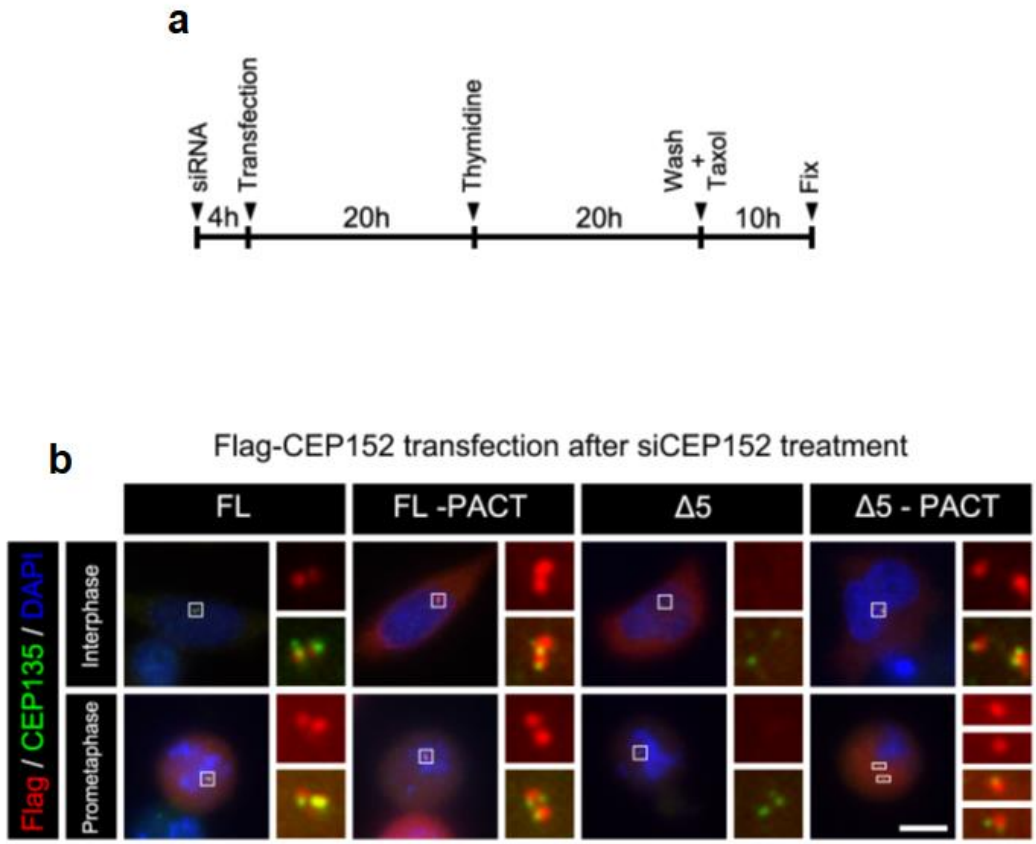

Figure 24. Centrosomal localization of the truncated Flag-CEP152-PACT proteins after transient transfection (**a**) Endogenous CEP152 was depleted in HeLa cells and the Flag-CEP152-PACT proteins were transiently transfected followed by sequential treatment of thymidine and Taxol. (**b**) HeLa cells were fixed and coimmunostained with antibodies specific to Flag (red) and CEP135 (green). DNA was visualized by DAPI (blue). Scale bar, 10 μm.

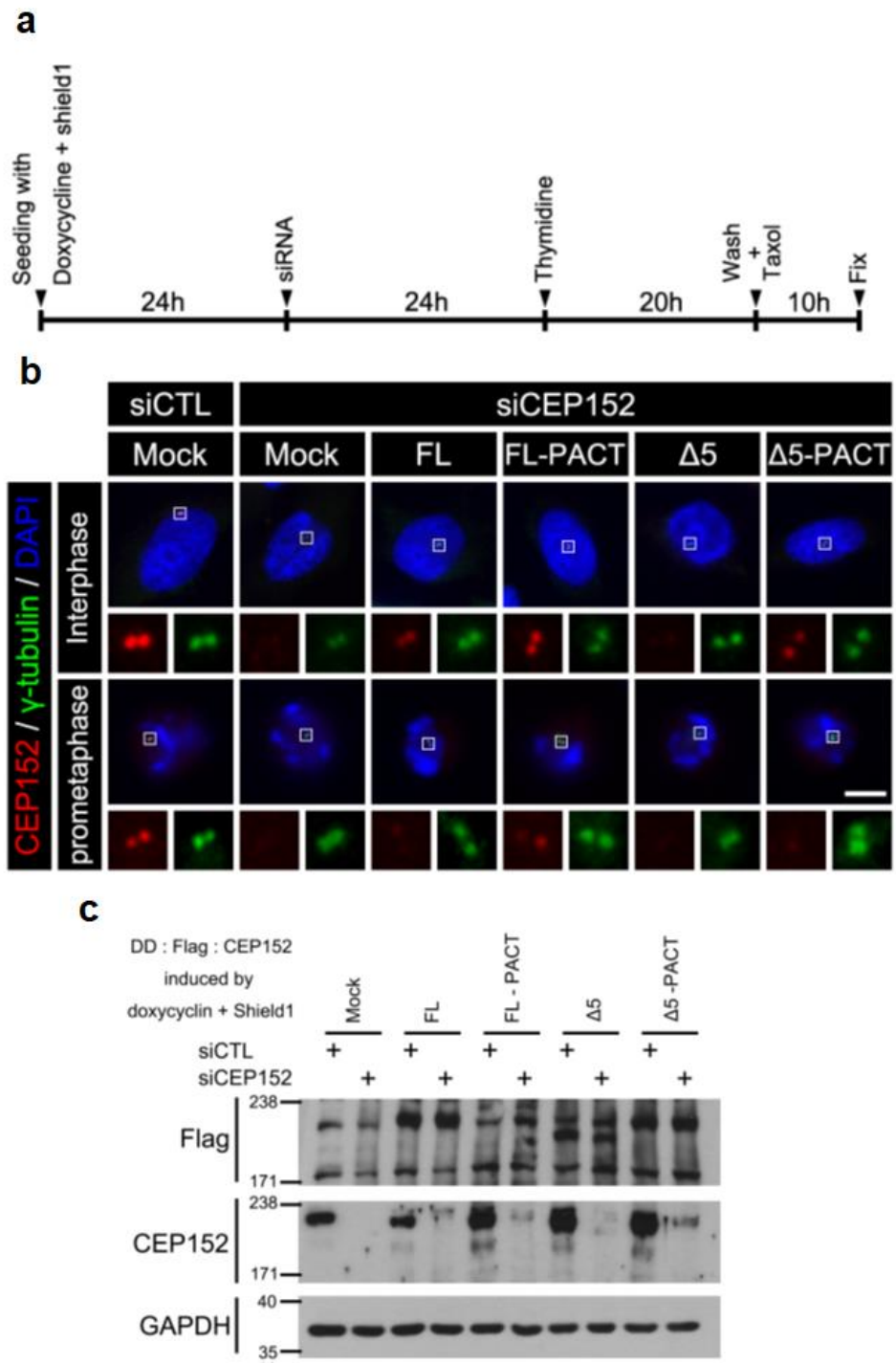

Figure 25. Centrosomal localization of the truncated Flag-CEP152-PACT proteins in stable cell lines

Figure 25. Centrosomal localization of the truncated Flag-CEP152-PACT proteins in stable cell lines (**a**) The truncated Flag-CEP152-PACT constructs were expressed by combination of doxycycline and shield1. Endogenous CEP152 was depleted by siCEP152 treatment and cells were arrested at prometaphase by sequential treatment of thymidine and Taxol. (**b**) All cells in every established cell line were fixed and coimmunostaining was performed with the CEP152 (red), γ-tubulin (green) antibodies. DNA was visualized with DAPI (blue). Scale bar, 10 μm. (**c**) The cells in every stable cell line group were harvested for immunoblot analysis with indicated antibodies.

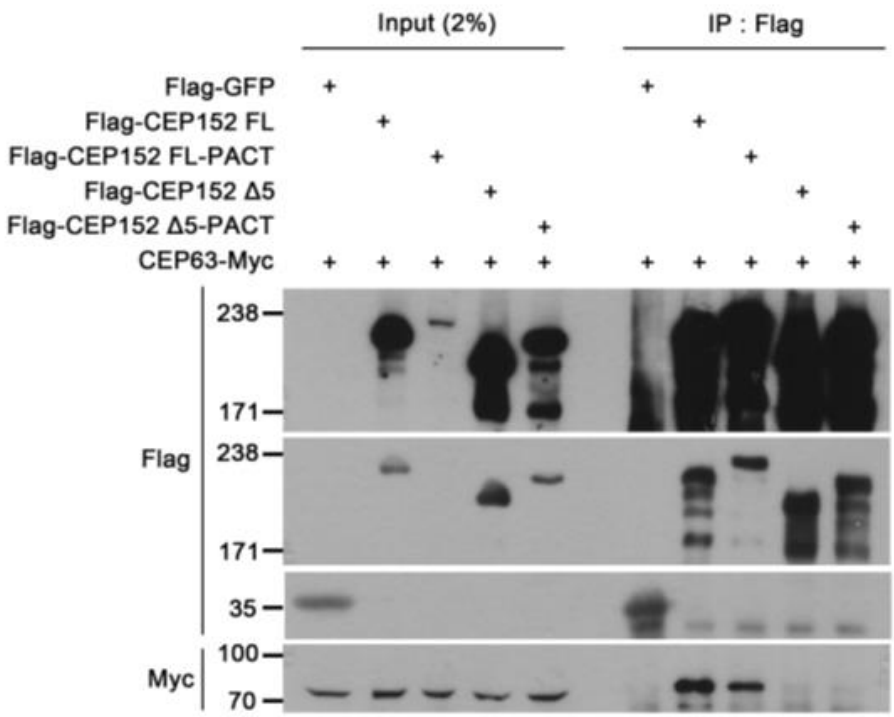

Figure 26. Interaction of the Flag-CEP152-PACT with the CEP63-Myc HEK 293T cells were harvested in 24 h after co-transfection of the CEP63-Myc and indicated Flag-CEP152-PACT proteins. The anti-FLAG M2 Agarose Bead was used for immunoprecipitation and immunoblot analysis was carried out with the Flag and Myc antibodies.

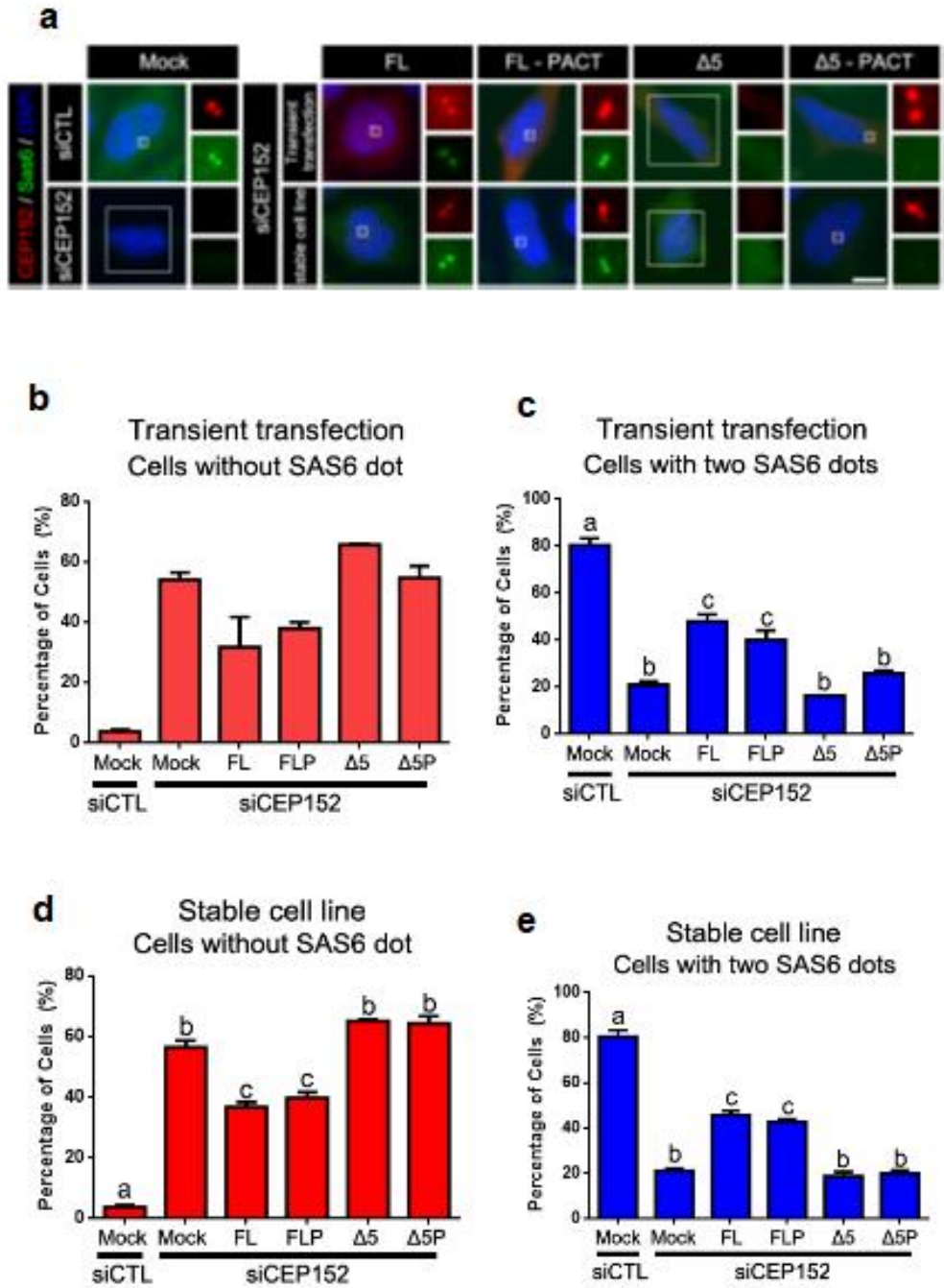

Figure 27. Determination of the centriole assembly activity in the Flag-CEP152-PACT-expressing cells

Figure 27. Determination of the centriole assembly activity in the Flag-CEP152-PACT-expressing cells (**a**) Cells were induced to express 4 different Flag-CEP152-PACT proteins by two means, transient transfection on HeLa cells and doxycycline induction on FRT/TO polyclonal stable cell lines. Coimmunostaining were performed in both conditions with antibodies specific to CEP152 (red) and SAS6 (green). DNA was visualized with DAPI (blue). Scale bar, 10 μm. (**b-e**) The number of SAS6 was counted in transient transfection condition (**b, c**) and stable cell line condition (**d, e**). Percentage of Cells with 0 SAS6 dots (**b, d**) and 2 SAS6 dots (**c, e**) were calculated. Values are means with standard error of the mean (SEM). n=200 per group in 2 independent experiments for (b, c) and n=300 per group in 3 independent experiment for (d, e). The statistical significance was determined by one-way ANOVA and Turkey's multiple comparison test in Prism 6 and was indicated by lower cases ($P<0.01$).

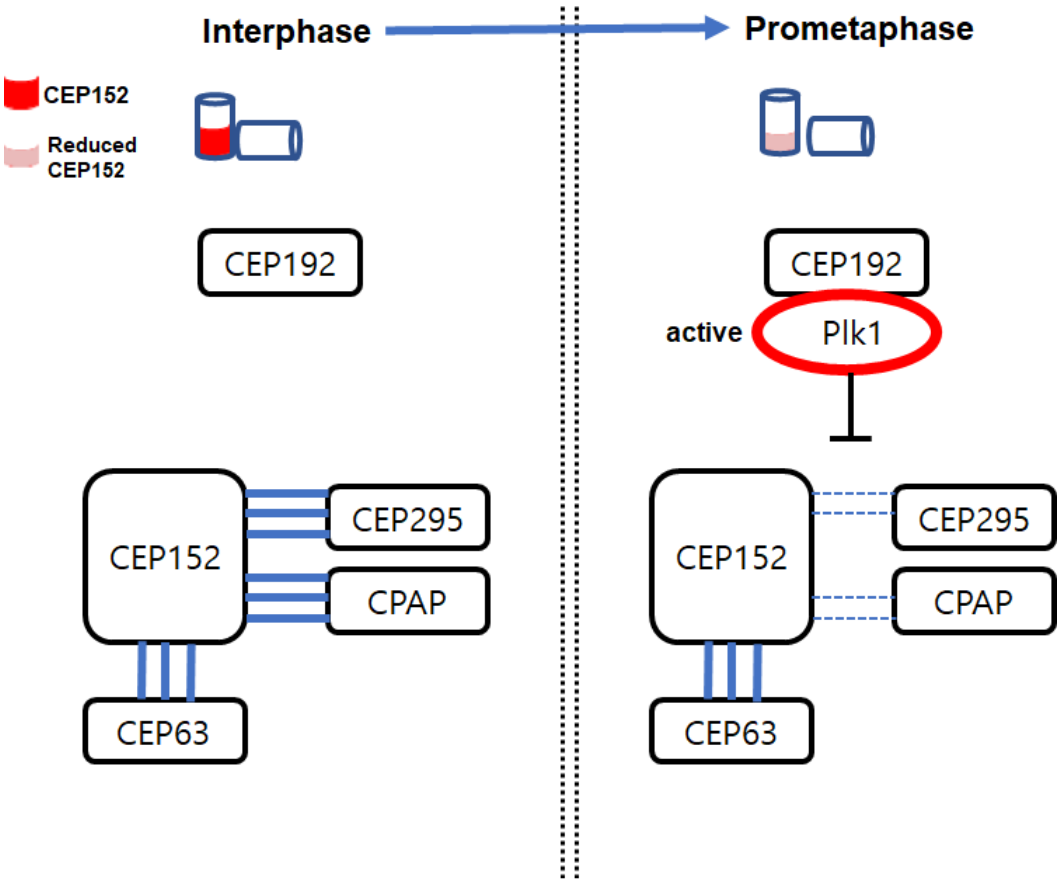

Figure 28. Model for the regulatory mechanism of centrosomal CEP152 level in mitosis Interaction between CEP63 and CEP152 is strong in interphase and mitosis, and this interaction is not inhibited by Plk1 activity. Centrosomal CEP152 level reduces with entering mitosis, because of the Plk1 kinase activated by CEP192 working as a platform. Phosphorylation by the plk1 weakens the CEP152 interactions with CEP295 and CPAP which makes centrosomal CEP152 level reduced.

REFERENCES

Banaszynski, L. A., Chen, L. chun, Maynard-Smith, L. A., Ooi, A. G. L. and Wandless, T. J. (2006). A Rapid, Reversible, and Tunable Method to Regulate Protein Function in Living Cells Using Synthetic Small Molecules. *Cell* **126**, 995–1004.

Bettencourt-Dias, M. and Glover, D. M. (2007). Centrosome biogenesis and function: Centrosomics brings new understanding. *Nat. Rev. Mol. Cell Biol.* **8**, 451–463.

Bornens, M. (2012). The centrosome in cells and organisms. *Science (80-.).* **335**, 422–426.

Brown, N. J., Marjanović, M., Lüders, J., Stracker, T. H. and Costanzo, V. (2013). Cep63 and Cep152 Cooperate to Ensure Centriole Duplication. *PLoS One* **8**, e69986.

Chalfie, M. and Kain, S. R. (2005). *Green Fluorescent Protein: Properties, Applications and Protocols: Second Edition*. (ed. Chalfie, M.) and Kain, S. R.) Hoboken, NJ, USA: John Wiley & Sons, Inc.

Chang, J., Cizmecioglu, O., Hoffmann, I. and Rhee, K. (2010). PLK2 phosphorylation is critical for CPAP function in procentriole formation during the centrosome cycle. *EMBO J.* **29**, 2395–2406.

Cizmecioglu, O., Arnold, M., Bahtz, R., Settele, F., Ehret, L., Haselmann-Weiß, U., Antony, C. and Hoffmann, I. (2010). Cep152 acts as a scaffold for recruitment of Plk4 and CPAP to the centrosome. *J. Cell Biol.* **191**, 731–739.

Conduit, P. T., Wainman, A. and Raff, J. W. (2015). Centrosome function and assembly in animal cells. *Nat. Rev. Mol. Cell Biol.* **16**, 611–624.

Dzhindzhev, N. S., Yu, Q. D., Weiskopf, K., Tzolovsky, G., Cunha-Ferreira, I., Riparbelli, M., Rodrigues-Martins, A., Bettencourt-Dias, M., Callaini, G. and Glover, D. M. (2010). Asterless is a scaffold for the onset of centriole assembly. *Nature* **467**, 714–718.

Egeler, E. L., Urner, L. M., Rakhit, R., Liu, C. W. and Wandless, T. J. (2011). Ligand-switchable substrates for a ubiquitin-proteasome system. *J. Biol. Chem.* **286**, 31328–31336.

Fu, J. and Glover, D. (2016). How the newborn centriole becomes a mother. *Cell Cycle* **15**, 1521–1522.

Fu, J., Lipinszki, Z., Rangone, H., Min, M., Mykura, C., Chao-Chu, J., Schneider, S., Dzhindzhev, N. S., Gottardo, M., Riparbelli, M. G., et al. (2016). Conserved molecular interactions in centriole-to-centrosome conversion. *Nat. Cell Biol.* **18**, 87–99.

Gheghiani, L., Loew, D., Lombard, B., Mansfeld, J. and Gavet, O. (2017). PLK1 Activation in Late G2 Sets Up Commitment to Mitosis. *Cell Rep.* **19**, 2060–2073.

Gillingham, A. K. and Munro, S. (2000). The PACT domain, a conserved centrosomal targeting motif in the coiled-coil proteins AKAP450 and pericentrin. *EMBO Rep.* **1**, 524–529.

Gönczy, P. (2012). *Towards a molecular architecture of centriole assembly*. Nature Publishing Group.

Gupta, G. D., Coyaud, É., Gonçalves, J., Mojarad, B. A., Liu, Y., Wu, Q., Gheiratmand, L., Comartin, D., Tkach, J. M., Cheung, S. W. T., et al. (2015). A Dynamic Protein Interaction Landscape of the Human Centrosome-Cilium Interface. *Cell* **163**, 1484–1499.

Habedanck, R., Stierhof, Y. D., Wilkinson, C. J. and Nigg, E. A. (2005). The Polo kinase Plk4 functions in centriole duplication. *Nat. Cell Biol.* **7**, 1140–1146.

Hardin, J., Bertoni, G. and Kleinsmith, L. (2012). *Becker's World of the Cell*. 8th ed. Pearson.

Hatch, E. M., Kulukian, A., Holland, A. J., Cleveland, D. W. and Stearns, T. (2010). Cep152 interacts with Plk4 and is required for centriole duplication. *J. Cell Biol.* **191**, 721–729.

Holland, A. J. and Cleveland, D. W. (2009). Boveri revisited: Chromosomal instability, aneuploidy and tumorigenesis. *Nat. Rev. Mol. Cell Biol.* **10**, 478–487.

Izquierdo, D., Wang, W. J., Uryu, K. and Tsou, M. F. B. (2014). Stabilization of cartwheel-less centrioles for duplication requires CEP295-mediated centriole-to-centrosome conversion. *Cell Rep.* **8**, 957–965.

Joukov, V., Walter, J. C. and De Nicolo, A. (2014). The Cep192-Organized Aurora A-Plk1 Cascade Is Essential for Centrosome Cycle and Bipolar Spindle Assembly. *Mol. Cell* **55**, 578–591.

Kim, K. and Rhee, K. (2011). The pericentriolar satellite protein CEP90 is crucial for integrity of the mitotic spindle pole. *J. Cell Sci.* **124**, 338–347.

Kim, S. and Rhee, K. (2014). Importance of the CEP215-pericentrin interaction for centrosome maturation during mitosis. *PLoS One* **9**, e87016–e87016.

Kim, K., Lee, S., Chang, J. and Rhee, K. (2008). A novel function of CEP135 as a platform protein of C-NAP1 for its centriolar localization. *Exp. Cell Res.* **314**, 3692–3700.

Kim, J., Kim, J. and Rhee, K. (2019a). PCNT is critical for the association and conversion of centrioles to centrosomes during mitosis. *J. Cell Sci.* **132**, jcs225789.

Kim, T. S., Zhang, L., Il Ahn, J., Meng, L., Chen, Y., Lee, E., Bang, J. K., Lim, J. M., Ghirlando, R., Fan, L., et al. (2019b). Molecular architecture of a cylindrical self-assembly at human centrosomes. *Nat. Commun.* **10**, 1151.

Kitagawa, D., Vakonakis, I., Olieric, N., Hilbert, M., Keller, D., Olieric, V., Bortfeld, M., Erat, M. C. M. C., Flückiger, I., Gönczy, P., et al. (2011). Structural basis of the 9-fold symmetry of centrioles. *Cell* **144**, 364–375.

Kollman, J. M., Merdes, A., Mourey, L. and Agard, D. A. (2011). Microtubule nucleation by γ-tubulin complexes. *Nat. Rev. Mol. Cell Biol.* **12**, 709–721.

Lattao, R., Kovács, L. and Glover, D. M. (2017). The centrioles, centrosomes, basal bodies, and cilia of Drosophila melanogaster. *Genetics* **206**, 33–53.

Lawo, S., Hasegan, M., Gupta, G. D. and Pelletier, L. (2012). Subdiffraction imaging of centrosomes reveals higher-order

organizational features of pericentriolar material. *Nat. Cell Biol.* **14**, 1148–1158.

Lee, K. and Rhee, K. (2012). Separase-dependent cleavage of pericentrin B is necessary and sufficient for centriole disengagement during mitosis. *Cell Cycle* **11**, 2476–2485.

Lindon, C. and Pines, J. (2004). Ordered proteolysis in anaphase inactivates Plk1 to contribute to proper mitotic exit in human cells. *J. Cell Biol.* **164**, 233–241.

Lončarek, J., Hergert, P. and Khodjakov, A. (2010). Centriole reduplication during prolonged interphase requires procentriole maturation governed by plk1. *Curr. Biol.* **20**, 1277–1282.

Lukinavičius, G., Lavogina, D., Orpinell, M., Umezawa, K., Reymond, L., Garin, N., Gönczy, P. and Johnsson, K. (2013). Selective chemical crosslinking reveals a Cep57-Cep63-Cep152 centrosomal complex. *Curr. Biol.* **23**, 265–270.

Matsuo, K., Ohsumi, K., Iwabuchi, M., Kawamata, T., Ono, Y. and Takahashi, M. (2012). Kendrin is a novel substrate for separase involved in the licensing of centriole duplication. *Curr. Biol.* **22**, 915–921.

Nigg, E. A. (2007). Centrosome duplication: of rules and licenses. *Trends Cell Biol.* **17**, 215–221.

Novak, Z. A., Conduit, P. T., Wainman, A. and Raff, J. W. (2014). Asterless licenses daughter centrioles to duplicate for the first time in Drosophila embryos. *Curr. Biol.* **24**, 1276–1282.

Novak, Z. A. A., Wainman, A., Gartenmann, L. and Raff, J. W. W. (2016). Cdk1 Phosphorylates Drosophila Sas-4 to Recruit Polo to Daughter Centrioles and Convert Them to Centrosomes. *Dev. Cell* **37**, 545–557.

Park, S. Y., Park, J. E., Kim, T. S., Kim, J. H., Kwak, M. J., Ku, B., Tian, L., Murugan, R. N., Ahn, M., Komiya, S., et al. (2014). Molecular basis for unidirectional scaffold switching of human Plk4 in centriole biogenesis. *Nat. Struct. Mol. Biol.* **21**, 696–703.

Sonnen, K. F., Gabryjonczyk, A.-M., Anselm, E., Stierhof, Y.-D. and Nigg, E. A. (2013). Human Cep192 and Cep152 cooperate in Plk4 recruitment and centriole duplication. *J. Cell Sci.* **126**, 3223–3233.

Tsou, M. F. B., Wang, W. J., George, K. A., Uryu, K., Stearns, T. and Jallepalli, P. V (2009). Polo Kinase and Separase Regulate the Mitotic Licensing of Centriole Duplication in Human Cells. *Dev. Cell* **17**, 344–354.

Tsuchiya, Y., Yoshiba, S., Gupta, A., Watanabe, K. and Kitagawa, D. (2016). Cep295 is a conserved scaffold protein required for generation of a bona fide mother centriole. *Nat. Commun.* **7**, 12567.

Wang, W. J., Soni, R. K., Uryu, K. and Tsou, M. F. B. (2011). The conversion of centrioles to centrosomes: Essential coupling of duplication with segregation. *J. Cell Biol.* **193**, 727–739.

Wang, G., Jiang, Q. and Zhang, C. (2014). The role of mitotic kinases in coupling the centrosome cycle with the assembly of the mitotic spindle. *J. Cell Sci.* **127**, 4111–4122.

Watanabe, K., Takao, D., Ito, K. K., Takahashi, M. and Kitagawa, D.

(2019). The Cep57-pericentrin module organizes PCM expansion and centriole engagement. *Nat. Commun.* **10**, 931.

Wheway, G., Nazlamova, L. and Hancock, J. T. (2018). Signaling through the Primary Cilium. *Front. Cell Dev. Biol.* **6**, 8.

국문초록

중심체는 모체중심립과 딸중심립, 그리고 중심구로 이루어진 세포소기관이다. 하나의 모체중심립에서는 하나의 딸중심립만이 형성될 수 있고, 이것은 중심체 수를 조절하는 중요한 기작이다. 이때 형성된 딸중심립은 중심립-중심체 전환과정을 거쳐야 모체중심립이 되어 새로운 딸중심립을 형성할 수 있다.

본 연구에서 집중하고 있는 CEP152는 새로운 중심립의 형성을 시작하는데 중요하며, 전환과정이 끝난 중심립에만 위치할 수 있다. 중심립-중심체 전환이 G1기에 일어나고 중심립의 합성은 S기부터 일어나기 때문에, 현재까지의 CEP152에 대한 대부분의 연구는 세포분열기를 벗어난 시점에 집중되어 있었다. 본 연구에서는 세포분열기의 초기에 집중하여 Plk1에 의한 CEP152의 중심체 집적 조절에 대해 관찰하였다. 또한 중심체 집적에 관여하는 CEP152의 상호작용 부위가 세포분열기에 들어가면서 달라지는 것을 관찰했으며, CEP152와 상호작용 단백질 간의 결합도가 세포주기에 따라 변하는 것을 관찰했다. 본 연구는 이 관찰결과들을 통해 CEP152의 중심체 집적도가 세포분열기에 들어가며 조절되는 과정에 대한 가설을 제시한다. 더 나아가, 이러한 세포분열기 초기의 조절과정이 세포분열기를 벗어난 이후의 중심립-중심체 전환과정에도 연관되어 있을 가능성을 제시한다.